ADDIS ABABA UNIVERSITY

ADDIS ABABA INSTITUTE OF TECHNOLOGY

SCHOOL OF MECHANICAL AND INDUSTRIAL ENGINEERING

Contact Stress Analysis and Surface Fatigue Life Estimation of Involute Spur Gear by Finite Element Method (FEM)

A Thesis Submitted to the Addis Ababa Institute Technology, School of Graduate Studies, Addis Ababa University

In Partial Fulfillment of the Requirement for Degree of Master of Science In Mechanical Engineering (Mechanical Design Stream)

By

Shiferaw Damtie Beyene

Advisor: Dr. Daniel Tilahun

September, 2014

Acknowledgment

I would like to thank Almighty God for giving me endurance for completion of this thesis. I would like to extend my sincere gratitude to my advisor Dr. Daniel Tilahun, for all of his help starting from giving an idea of different areas on his expertise while selecting the title of the theses at the beginning and continues guidance till the completion inspite of a lot of responsibilities he had as a School Dean.

Abstract

The main objective of this thesis is to analyze contact stress and estimate surface fatigue life in rolling-sliding contact of involute spur gear by finite element method (FEM). To do this three dimensional involute spur gear pair was developed in Solidworks 2012 Premium. This 3D model was imported to Ansysworkbench 14.5. FEM analysis was done after assigning displacement, load and support boundary conditions. The contact stress is analyzed and surface fatigue life is estimated. The results show that the contact stress in involute spur gear is agreeable with analytical contact stress by Hertz stress and the trend shows the error will decrease with higher load application. The contact stress also increases with higher friction in the area of contact .The surface fatigue life of involute spur gear was estimated using FEM and the result shows better surfaces which has less roughness result in high fatigue strength of the gear.

Contents

List of Figures

List of Tables

Chapter One

1. Introduction

1.1 Background of the project

Gears are most common for transmission of power from one machine to the other. In the design viewpoint, the fatigue strength and wear are the most important criteria because each gear tooth may experience billions of load cycles.

Fatigue failure of gears can lead to the catastrophic failure of equipment, taking into account that gears are important elements in the power transmission systems of many modern machines. Because of this, effective procedures and information to evaluate the load capacity and useful life of gears are needed by specialists in several fields of engineering application, including those involved with disaster preparedness and management in the fields of transportation, power generation, and the mechanical industry. The actual practice of engineering and increase of the work speeds in current applications of gears has required better specification of steel fatigue behavior for numbers of cycles greater than 10^6. In this sense, AGMA Standard 2105-D04 has introduced useful information to consider the fatigue load capacity of steel gears in the case of a high number of cycles.

When mechanical machinery move in periodical motion, stresses to the metal surfaces occur, often leading to the fatigue of a material. All repeating stresses in a rolling or sliding contact can give rise to fatigue failure. These effects are mainly based on the action of stresses in or below the surfaces, without the need of direct physical contact of the surfaces under consideration. When two surfaces slide across each other, the maximum shear stress lies some distance below the surface, causing micro cracks, which lead to failure of the component. These cracks initiate from the point where the shear stress is maximum, and propagate to the surface as shown in Figure 1.1

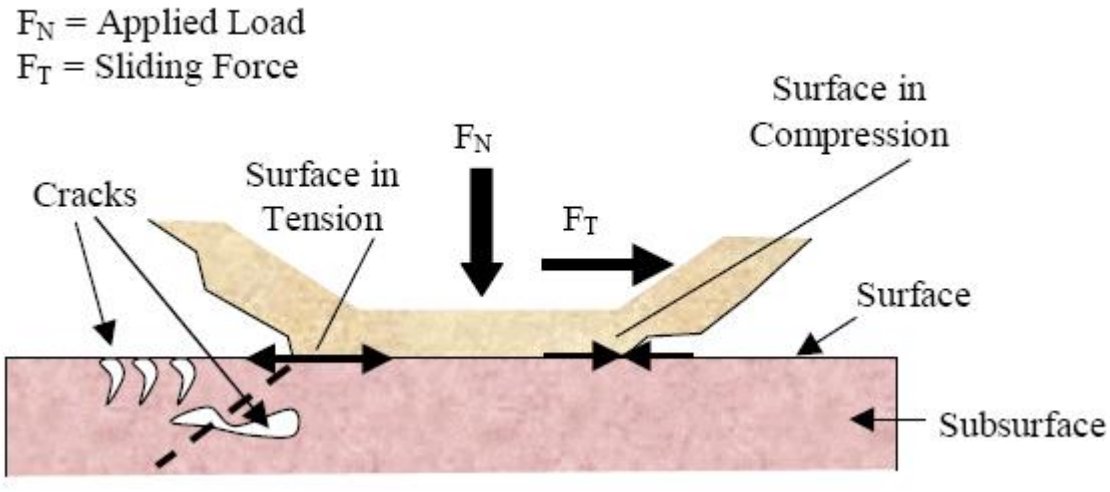

Figure 1.1Schematic of fatigue wear, due to the formation of surface & subsurface cracks [4]

Gears are subjected to rolling-sliding contact, for the spur gear, the contact between two teeth follows the line of action, as is illustrated in Fig. 1.2a. On the driving wheel it starts at the tooth root and moves towards the top. For the following wheel the movement is reversed, that isfrom top to root. For the first half of the interaction, when the contact is located between the root and the pitch circle of the driving wheel, friction forces are directed towards the root of the driving tooth, counteracting the rotation, Fig.1.2b. When the contact passes the pitch circle, the friction forces change direction and acts with the rolling motion. For the following tooth the friction forces are directed in the opposite direction. Thus for the spur gear, relative motion is constant across the contact width but variable through the interaction. The distribution of the relative velocity over the driving gear tooth is displayed in Fig. 1.2c.

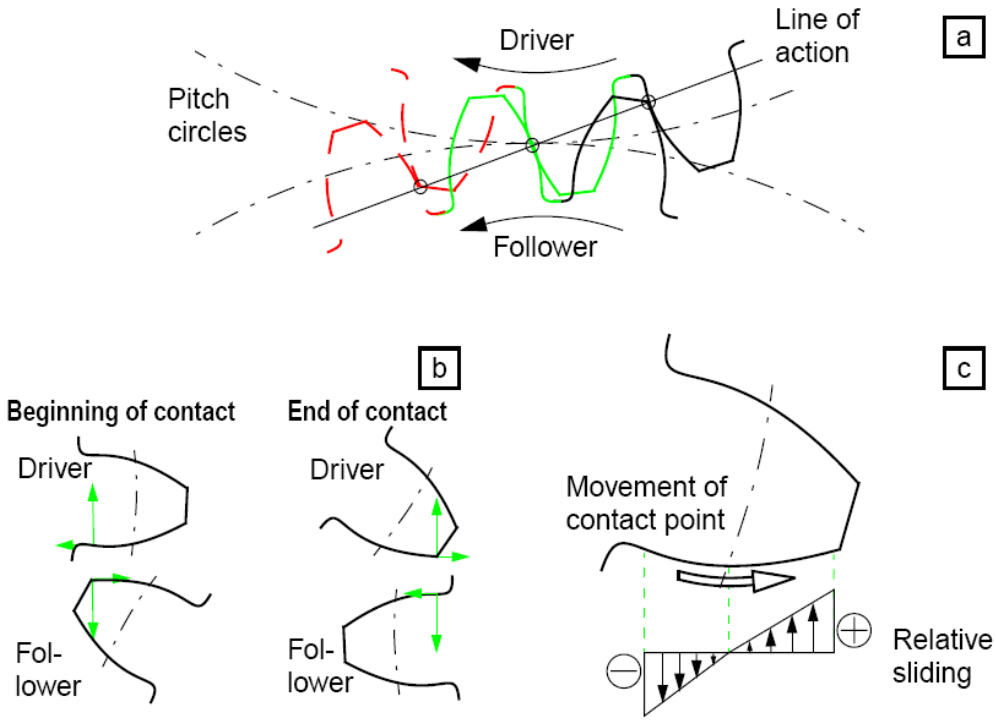

Figure 1.2 Contact of an involute spur gear: a) movement of the contact point, b) contact forces before and after the contact passes the pitch line and c) the distribution of relative contact velocity for the driving gear tooth [5].

As seen in Figure 1.2, gears are subjected to repeated rolling sliding contact which results in surface fatigue failure. Most of the researches which has been done are of experimental which is time taking and costly. A finite element based simulation for the estimation of surface fatigue life is emerging and getting greater attention.

1.2 Problem Statement

Several classical standardized procedures (DIN, AGMA, ISO, etc.) can be used for the approximate determination of load capacity of gear tooth root. They are commonly based on the comparison of the maximum tooth-root stress with the permissible bending stress [3]. Their determination depends on a number of different coefficients that allow for proper consideration of real working conditions (additional internal and external dynamic forces, contact area of engaging gears, gear's material, surface roughness, etc.). The classical procedures are exclusively based on

the experimental testing of the reference gears, and they consider only the final stage of the fatigue process in the gear tooth root, i.e. the occurrence of final failure.

The biggest drawback with experimental method is that it cannot be undertaken until a prototype exists. If a design problem then occurs it is usually very difficult to rectify. It is also very expensive to perform fatigue tests. For these reasons FEA based fatigue analysis has been perceived as an excellent enhancement to the experimental method.

1.3 Research Questions

The study will try to answer the following questions:

- How to simulate the 2D and 3D involute spur gear by FEA?
- How to find the contact stress in FEA?
- To what extent the FEA is similar to contact stress from Hertizean theory?
- Is surface conditions` affect surface fatigue life of spur gears?
- How to determine the surface fatigue life analytically?
- How to determine the surface fatigue life by FEM?
- Is a result from the FEM simulation will be agreeable with experimental method?

1.4 Objective

1.4.1. General Objective:

The general objective of this research is:

- To analyze contact stress and estimate surface fatigue life in rolling – sliding contact of involute spur gear by finite element method.

1.4.2. Specific objective:

The specific objectives are:

- To model 2D and 3D involute gear by modelling soft wares such as ,solid works , Auto desk inventor.
- To study the effect of loading conditions on surface fatigue strength of involute spur gear.
- To study the effect of surface finish on fatigue life by finite element method

- To verify the FEM with analytical method

1.5 Methodology

The contact stress analysis and surface fatigue estimations of spur gears which was done by experimental methods will be collected. The 2D and 3D models of the involute spur gear will be developed by modeling softwares such as Proe, Autodesk Inventor, Solid works and the FEM simulation will be done by Finite element softwares such as Ansys. The result will be compared with analytical methods.

1.6 Significance of the study

It is very expensive to perform contact stress analysis and fatigue tests experimentally, more over the experimental set ups may not be available in developing countries such as Ethiopia. Contact stress analysis and surface fatigue estimation of gears in FEM analysis will have several advantages over experimental methods. It can be used in areas where experimental setups are not available. Moreover we do the analysis quite a short time and we can predict the influence of different parameters such as initial surface roughness, temperature etc. It is also used to verify experimental results.

1.7 Scope and limitation of the research

The scope of this research is to perform parametric study to investigate the effect of loading condition and material types in contact stress in gears and FEM simulation to study the effect of surface fatigue on life of involute spur gear in rolling-sliding contact due to variation of surface roughness. The analysis will be done in ordinary computers hence to minimize computational time miniaturized gears will be used for the analysis in FEM.

1.8 Organization of the thesis

This thesis is organized in to five chapters. In the first chapter background, statement of the problem, research questions, objectives and significance of the study and scope are discussed. In chapter two a survey of literatures related to the research have been investigated. In chapter three materials used, dimensions and methods of analytical and FEM for contact stress and surface

fatigue life estimation have been discussed. In chapter four results found were discussed and finally chapter five the conclusions, recommendations and future work are given.

Chapter Two

2. Literature Review

A large number of researches has been done on gear modeling and analysis. The gear stress analysis, the transmission errors, and the prediction of gear dynamic loads, gear noise, and the optimal design for gear sets are always major concerns in gear design. For doing those analysis many mathematical models of gears have been developed for different purposes in stress analysis. The models are either a single tooth or a tooth pair model. Single tooth models are mostly used for tooth stress analysis however tooth pair analysis are mostly used for contact stress analysis. Finite element method is widely used for analysis of gear tooth. Ravichandra [10] studied the effect of rim thickness on gear tooth bending stress by finite element modeling approach.

M. Raja Roy et.al.[11] studied the trend of Maximum allowable Contact Pressure on involute pair of spur gear teeth decreases with increase in module and concluded that both analytical and finite element analysis by ansys follow same trend that is contact pressure decreases with increase in module.

Nakanishi et.al [14] studied the influence of surface texture and lubricating oil temperature on surface failure of rolling-sliding contact in the case of case-carburized alloy steel. this study is experimental and found that the case carburized gears with the higher surface durability can be developed by functioning and smooth tooth surface and controlling the lubrication.

Ali Raad Hassan [13] analyzes contact stress, considering contact ratio, approach angle, recess angle, contact and length of contact. It was found that stress was more than the correct value of contact stress obtaining from approximating tools. This search was carried out with the help of finite element analysis which could be difficult to do otherwise. A computer program was developed to plot one pair of teeth in contact at different positions of contact depending on the formulation. Ten different positions were taken at intervals of three degree and the corresponding ten finite models and finite element analysis was done. On this study it is found that the maximum stress occurs in a single tooth contact position and less stress before and after this position. Parveen Kumar, Harsh Raghuvanshi [14] analyse the effect of geometric conditions: gear ratio, normal

module and face width on the failure load and beam strength is done. The stress analysis is done by using solidworks.

Vivek K. et.al. [15] compared the theoretical maximum contact stress calculated by Hertz equation and the finite element analysis of spur gear done to determine the maximum contact stress by ANSYS 14.5. Two gear materials steel and grey cast iron was used and found that the results from both Hertz equation and Finite Element Analysis are comparable.

Atul Kumar et.al. [23] presented the use of reverse engineering in assessing the gear tooth stress and in turn the remaining life of a wear out gear. 3D CAD geometric models were reconstructed before wear and after wear for gear using reverse engineering technology. Finite element numerical simulation is implemented for the rebuilt spur gear CAD model, and the peak values as well as the locations of stress and deformation are analyzed on gear tooth. With the help of FEA results and AGMA equations one can evaluate the remaining life of the gear, accordingly operating condition of the gear train can be modified and improved to get more remaining life of the gear train.

Gang Deng et.al.[24] developed an empirical method to evaluate the surface strength of a rolling-sliding surface such as traction drive rollers and gears where the surface temperature rise is very high for high speed and heavy load. The authors suggest introducing the surface temperature to the surface strength evaluation. In this paper, the surface temperature measurements were performed on rollers, and the effects of load, sliding velocity and mean tangential velocity as well as surface roughness on surface temperature were evaluated. An approach to use the surface temperature index in the surface fatigue strength evaluation was attempted. The found that an experimental equation was presented for the calculation of surface temperature based on the surface temperature measurement results. The applicability of the equation to the other kinds of rollers and gears was confirmed. More over the effects of load, sliding velocity, mean tangential velocity and surface roughness on surface temperature are evaluated by a surface temperature index, which might be useful in surface fatigue evaluation.

Amisha Y. Pathak [25] studied contact fatigue of gear teeth flanks, a general computational model for the determination of initiation fatigue loading cycles in meshing gears. An equivalent contact model of a cylinder and flat surface is used for the simulation of contact fatigue crack initiation

under conditions of rolling and sliding contact loading of meshing gears. The material model is as summed to be homogenous, without imperfections and/or inclusions, and elastic shakedown is considered. The modified Coffin -Manson method, in the frame work of finite element analysis (FEM), is used for iterative analyses of contact fatigue crack initiation.

Ravichandra Patchigolla and Yesh P. Singh [27], used Finite element based approach was used to investigate the effect of the gear rim thickness on the tooth bending stresses in large spur gears. A program was developed using ANSYS Parametric Design Language (APDL), which can generate two dimensional or three dimensional finite element model of 1, 3 or 5 teeth segment with user defined rim thickness value. Models were constrained on the radial sides in the rim portion and also on the nodes located circumferentially along the bottom surface at the rim-web interface. The models are studied for the case of full load acting at Highest Point of Single Tooth Contact (HPSTC). A different meshing approach was developed in the generation of finite element grid.

G. Mallesh, et.al. [28]. Generated asymmetric spur gear tooth profile for different pressure angles on drive and coast sides and estimate the critical section using C- programming. Bending stress analysis has been performed using finite element analysis using ANSYS software .Comparison of bending stress analysis has been performed for symmetric and asymmetric spur gear tooth at critical section.

Muhsi n J. Jweeg et.al. [29] used 2D contact stress FEA model to simulate contact between two bodies accurately by verification of contact stresses between two gears in contact . And they concluded the module has the greater effect on the behavior of the tooth contact stresses: Decreasing the module leads to increase in the contact stress. Increasing the spur gear design parameters (pressure angle, number of teeth and module) leads to improvement in the tooth strength by increasing the thickness of the critical section which results in increasing the area of tooth critical section and makes it able to withstand higher loads.

Timothy Krantz et.al. [30] Gears made from steel alloy Ferrium C69 were tested using the NASA Glenn Research Center's gear test apparatus. Their study result were compared to past works done using the same test apparatus and test methods. For surface fatigue testing, the results were compared to previous works testing AISI 9310 and Pyrowear 53 (AMS 6308B), two alloys used in production today as aircraft steels. Surface fatigue testing was done at a contact stress of 1.7 GPa.

The Ferrium C69 provided for better surface fatigue performance relative to the production alloys. For bending fatigue testing, the results were compared to previous works testing AISI 9310. Testing was completed using the single tooth bending method, load control, and a crack initiation definition of a 2 percent increase in the test load stroke relative to the stroke of the initial loadings. Tests were conducted at loads that generally resulted in crack initiation in the cycle range 100 cycles to 1 million.

Fukuoka K.[9] An examination of optimization of the surface hardening process using a recently developed dual phase steel was carried out with the aims of improving fatigue strength and reducing heat-treatment distortion. The following results were obtained. An improvement of 29% in pitting fatigue strength was obtained in comparison with the conventional SCM822H gas-carburized material by using the dual phase steel and optimizing the surface hardening process; Of the 29% improvement in pitting fatigue strength, 9% was attributed to the improvement effect of changing the steel from SCM822H to the dual phase steel; A 12% improvement effect was obtained by changing the surface hardening process from the conventional gas carburizing to vacuum carbonitriding. In addition, fatigue strength was improved by 7% by performing double shot peening.

Chapter Three

3. Analytical Methods in contact stress analysis and surface fatigue life estimation of involute spur gear

3.1 Gear Materials

List of materials and their characteristics used for the study are shown in Table 3.1

Table 3.1 List of materials and their characteristics

Material	Bulk modulus of Elasticity	Poisson's ratio
Chromium-molybdenum alloy steel (SCM 420)	**206**	**0.3**
Grey cast iron GG-20	**91**	**0.25**
Grey cast iron GG-25	**105**	**0.25**
Grey cast iron GG-30	**113**	**0.25**
Structural steel	**200**	**0.3**

3.2 Spur Gear Dimensions

3.2.1 Basic Nomenclatures and Gear Tooth Terminology of spur gear

The basic terms associated with spur gears and spur gearing systems are defined below. (see Figure.3.1 and Figure 3.2)

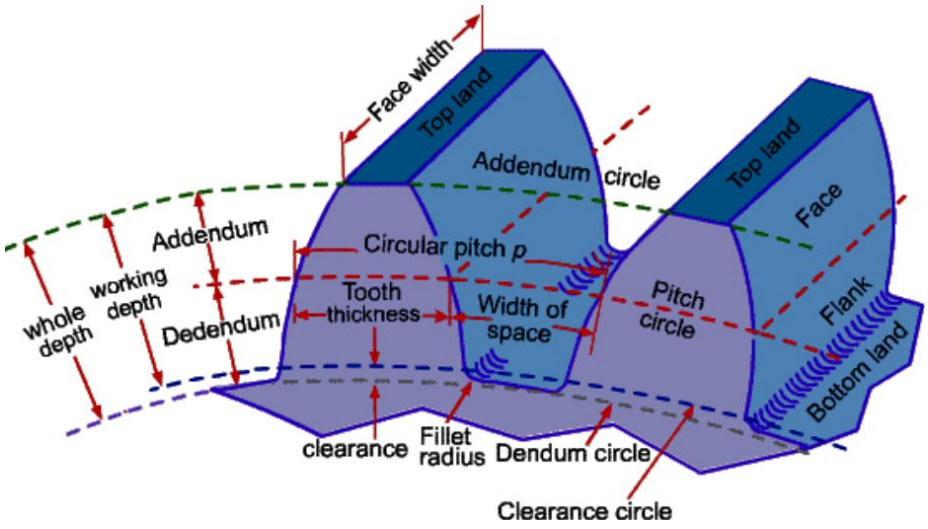

Figure.3.1 Basic gear geometry [26]

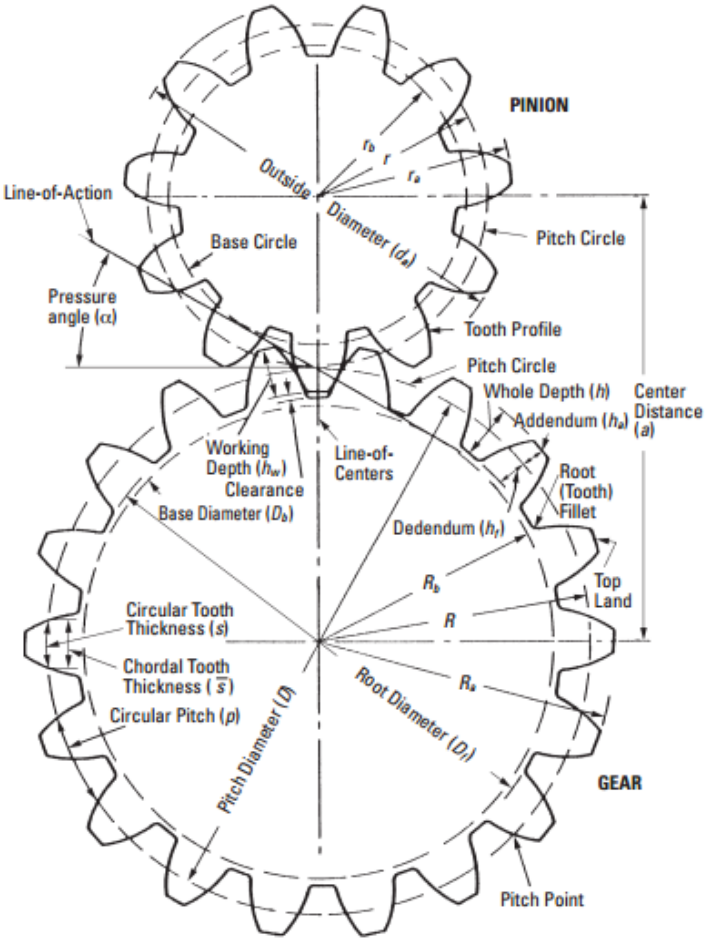

Figure.3.2. Basic gear geometry meshed gears [20]

Pitch surface: The surface of the imaginary rolling cylinder (cone, etc.) that replaces the toothed gear.

Pitch circle: A normal section of the pitch surface.

Addendum circle: A circle bounding the ends of the teeth, in a normal section of the gear.

Dedendum circle or Root circle: The circle bounding the spaces between the teeth, in a normal section of the gear.

Addendum: The radial distance between the pitch circle and the addendum circle.

Dedendum: The radial distance between the pitch circle and the root circle.

Clearance: The difference between the dedendum of one gear and the addendum of the mating gear.

Face of a tooth: That part of the tooth surface lying outside the pitch surface.

Flank of a tooth: The part of the tooth surface lying inside the pitch surface.

Top land: The top surface of a gear tooth.

Bottom land: The bottom surface of the tooth space.

Circular thickness (tooth thickness): The thickness of the tooth measured on the pitch circle. It is the length of an arc and not the length of a straight line.

Tooth space: The space between successive teeth.

Width of space: The distance between adjacent teeth measured on the pitch circle.

Backlash: The difference between the tooth thickness of one gear and the tooth space of the mating gear.

Circular pitch p: The width of a tooth and a space, measured on the pitch circle. It is equal to the pitch circumference divided by the number of teeth. If,

Diametral pitch P: The number of teeth of a gear per unit pitch diameter. The diametral pitch is hence the number of teeth divided by the pitch diameter. In metric system, module is used instead of diametral pitch. It is nothing but the inverse of diametral pitch.

Module m: Pitch diameter divided by number of teeth. The pitch diameter is usually specified in millimeters.

3.2.2 Basic Gear dimensions

The equations for basic gear dimensions [6] are shown in Table 3.2

Table 3.2 Basic equations of gear dimensions

Parameter	Formulae
Module	$m = \frac{d}{n}$
Number of teeth	$n = \frac{d}{m}$
Base circle diameter	$D_b = d \times \cos\alpha$
Pitch circle diameter	$d = n \times m$ $\quad (d_g \text{ for gear and } d_p \text{ for pinion})$
Center distance	$a = \frac{(d_g + d_p)}{2}$
Outside diameter	$D_o = (n+2)m$
Circular pitch	$p = m\pi$
Deddendum	$h_f = 1.25m$
Addendum	$h_a = m$
Whole depth (min)	$h = 2.25m$

Based on the equations in Table 3.2 the specification of the pinion and gear used for this study is shown in Table 3.3.

Table 3.3 Specification of pinion and gear [7].

Parameters	**Pinion**	**Gear**
Material	Structural steel	Structural steel
No. of teeth	22	22
Module (mm)	3	3
Pitch circle diameter (mm)	66	66
Face width (mm)	7	7

3.3 Methods

3.3.1 Geometrical Modeling and Involute tooth profile generation

Consider that a planar curve I is given (Fig.3.3). Segments MiNi (i =1, 2,...,n) represent the curvature radii of curve I at points Mi, where Ni is the curvature center. The locus of curvature centers Ni is the evolute E to curve I. The main features of E, evolute to curve I, are as follows:

(i) The normal MiNi at point Mi of curve I is the tangent to the evolute E.

(ii) The evolute to a regular curve I is the envelope to the family of normals MiNi to I.

Considering E as given, we may determine the involute I for E as the result of development of E. Let us imagine an inextensible thread MN that is wrapped on curve E. Point M of the thread will trace out the involute I while the thread is wound on and off.

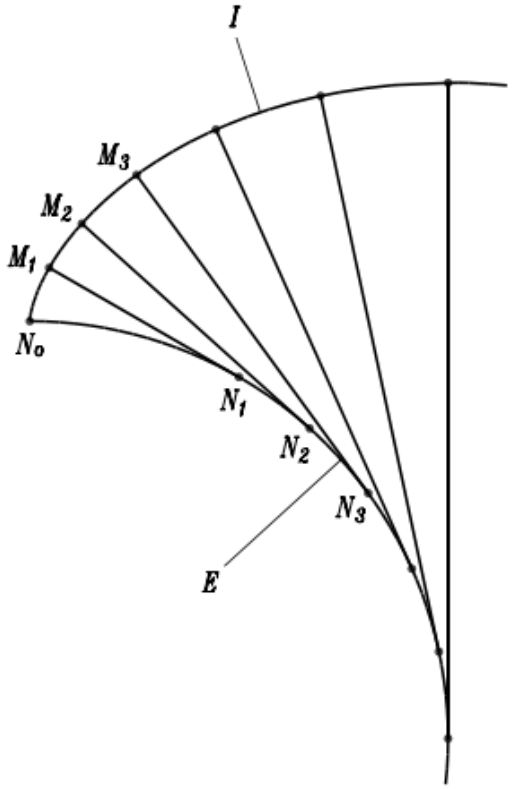

Figure 3.3. Evolute and Involute curves [22]

Consider the particular case when the evolute E is a circle. The involute I for such a case is the tooth profile for a spur gear. The circle of radius r_b (Fig. 3.4) is called the base circle. Two branches of an involute curve are shown in Fig. 3.4. They are generated by point Mo of the straight line that rolls over the base circle clockwise and counterclockwise, respectively. Each branch represents its respective side of the tooth (Fig. 3.5).

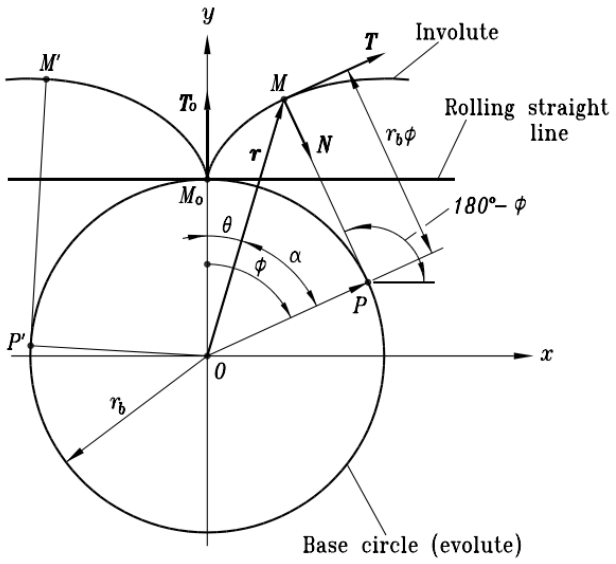

Figure 3.4 For derivation of the equation of an involute curve [22]

As it is seen in Figure 3.4, analytical representation of an involute curve is based on the following considerations.

(i) A current point M of the involute curve is determined by the vector equation

$$\overline{OM} = \overline{OP} + \overline{PM} \quad \text{.....(3.3.1)}$$

where

$$\overline{OP} = r_b[\sin\varphi \;\; \cos\varphi]^T \quad \text{.....(3.3.2)}$$

$$\overline{PM} = PM[-\cos\varphi \;\; \sin\varphi]^T \quad \text{.....(3.3.3)}$$

(ii) Due to rolling without sliding, we have

$$\overline{PM} = curve(M_0P) = r_b\varphi \quad \text{.....(3.3.4)}$$

Here, φ is the angle of rotation in rolling motion.

(iii) Equations (3.3.1) to (3.3.4) yield

$$\begin{aligned} x &= r_b(\sin\varphi - \varphi\cos\varphi) \\ y &= r_b(\cos\varphi + \varphi\sin\varphi) \end{aligned} \quad \text{.....(3.3.5)}$$

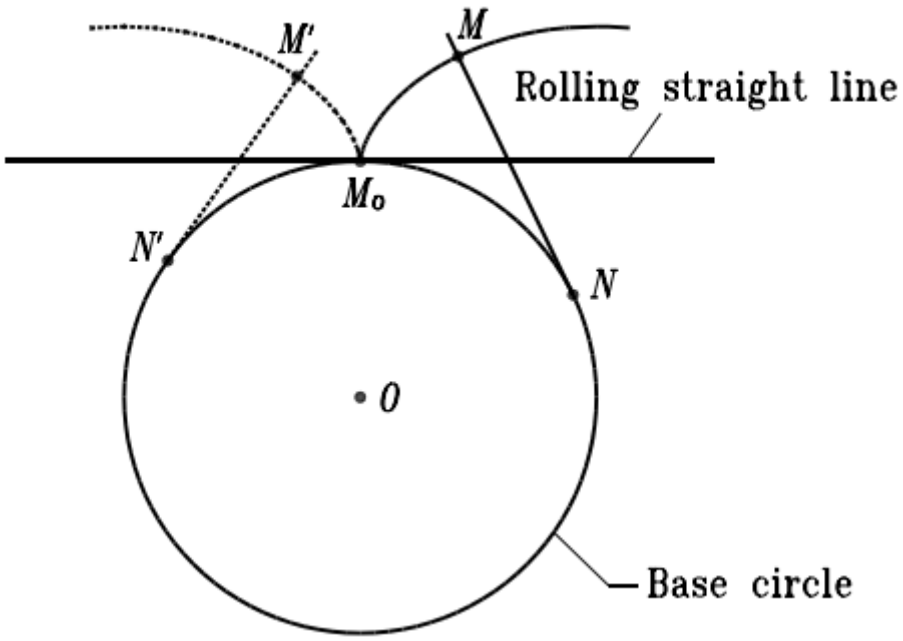

Figure 3.5 Two branches of an Involute curve [22]

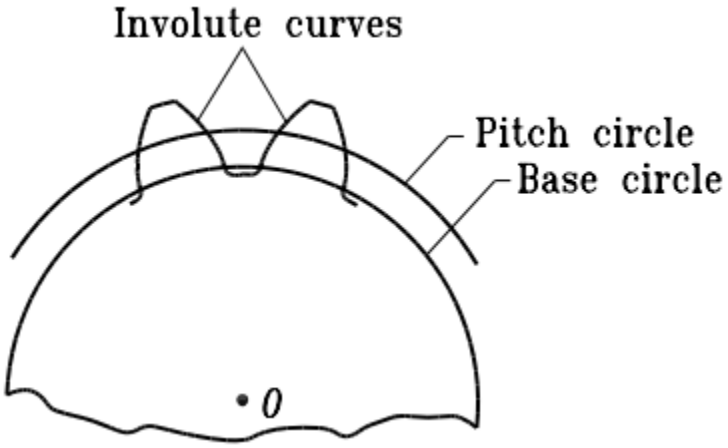

Figure 3.6 Two branches of an involute curve [22]

The involute equation can be given by:

$$\left.\begin{aligned} x(t) &= R\times[\cos(t)+t\times\sin(t)] \\ y(t) &= R\times[\sin(t)-t\times\cos(t)] \end{aligned}\right\} \quad \text{.....(3.3.6)}$$

Where R=pitch radius

t= angle parameter in radians

$x(t)$ is a function with respect to parameter t

$y(t)$ is a function with respect to parameter t

Using equation 3.3.6, a 2-D sketch of the involute spur gear is generated (Figure 3.12).this sketch is now extruded to a length equal to the face width of the gear which will give us a 3-D involute spur gear (Figure 3.13).

3.3.2 Analytical Methods in contact stress analysis

The study of deformation of solids which are in contact at one or more points is called Contact Mechanics. When two gears mesh, the region of contact is theoretically a line. The curvatures of the individual mating surfaces at the points of contact will vary according to the given dimensions of the tooth profile of the mating gears as well as to the instantaneous positions of the point of contact on the line of action as the gear tooth surfaces roll and slide during the course of action. The nature of contact is, therefore, analogous to that of two contacting cylinders of constantly changing radii of curvature. Though theoretically it is a line contact, the line actually develops into a band of certain width along the length of the teeth due to mutual compressive pressure. The stress pattern developed within this band is quite complicated. According to Dudley as cited in [17], this is what happens when the gear tooth surfaces are in action a point of maximum compressive stress is created in the centre of the hand of contact.

Contact stress is generally the deciding factor for the determination of the requisite dimensions of gears. Different research on gear action have confirmed fact that beside contact pressure, sliding velocity, viscosity of lubricant as well as other factors such as frictional forces also influence the formation of pits on the tooth surface. Thus the thorough study of contact stress between meshing gears is crucial in gear design. The German physicist, Heinrich Hertz, developed expressions for

the stresses which are created when two curved surfaces are in contact. These surface stresses are universally known as contact stresses or Hertz stresses or Hertzian stresses.

The classical theory of contact focused primarily on non-adhesive contact where no tension force is allowed to occur within the contact area, i.e., contacting bodies can be separated without adhesion forces. Several analytical and numerical approaches have been used to solve contact problems that satisfy the no-adhesion condition. Complex forces and moments are transmitted between the bodies where they touch, so problems in contact mechanics can become quite sophisticated. In addition, the contact stresses are usually a nonlinear function of the deformation. To simplify the solution procedure, a frame of reference is usually defined in which the objects (possibly in motion relative to one another) are static. They interact through surface tractions (or pressures/stresses) at their interface. The following assumptions are made in determining the solutions of Hertzian contact problems:

- The strains are small and within the elastic limit.
- The surfaces are continuous and non-conforming (implying that the area of contact is much smaller than the characteristic dimensions of the contacting bodies).
- Each body can be considered an elastic half-space.
- The surfaces are frictionless.

Additional complications arise when some or all these assumptions are violated and such contact problems are usually called non-Hertzian.

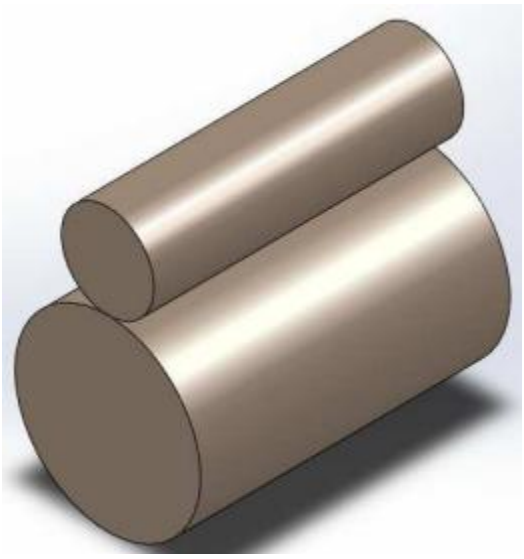

(a)

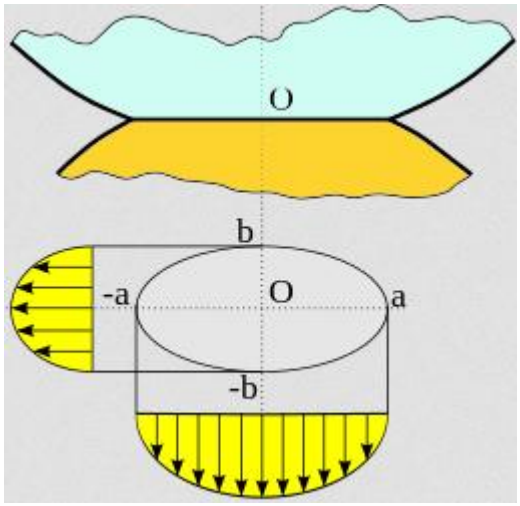

(b)

Figure 3.7 Contact between a) Cylinders b) Sphere

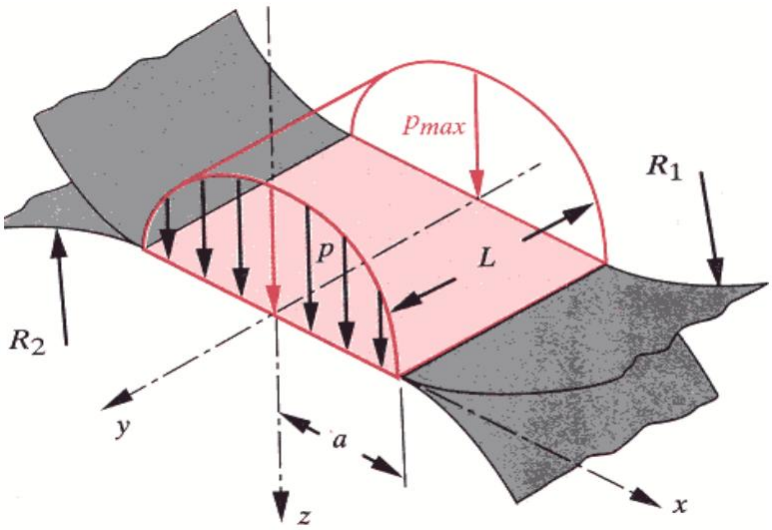

Figure 3.8. The Hertz pressure distribution of a two dimensional contact

The Cylinders used in this study are having a length L, d1 and d2 as diameters. On application of Force F, on the surfaces of the cylinders a narrow rectangle of width 2B and length L is generated at the contact surfaces. A pressure is developed in the rectangle area in an elliptical shape. The half width of the ellipse is given by

$$a = \sqrt{\frac{2F}{\pi L}\frac{\frac{(1-\nu_1^{\,2})}{E_1}+\frac{(1-\nu_2^{\,2})}{E_2}}{\frac{1}{d_1}+\frac{1}{d_2}}} \quad \text{.....(3.3.7)}$$

Where

- a is ellipse half width
- F is force acting on surface of cylinder
- L is length of cylinder
- d1 and d2 are diameters of cylinder

The meshing of two involute teeth have similar with the contact two cylinders or disks. Hence Hertz equation can be used to determine the contact stresses in the mating teeth of gear. Hertzian equation for contact stress in the teeth of mating gears is given by,

$$\sigma_c = \sqrt{\frac{F(1+\frac{R_1}{R_2})}{R_1 B\pi[\frac{(1-\vartheta_1^2)}{E_1}+\frac{(1-\vartheta_2^2)}{E_2}]\sin\phi}} \quad \text{.....(3.3.8)}$$

Where σ_c is the contact stress in mating teeth of spur gear, F is the force, R_1 and R_2 are pitch radii of two mating gears, B is the face width of gears, ϕ is the pressure angle, ϑ_1 and ϑ_2 , are the Poisson ratios E_1 and E_2 , are the moduli of elasticity of two gears in mesh.

Using equations which are description of the Hertz Contact Stress in involute spur gear, a basic computer program is performed using Matlab release 2010b. A computer programming code using Matlab is developed to compute contact stress by using Hertizean Formulae and plot the graphs is shown in Appendix I

Using the above code the Hertizean contact stress for different moments applied is shown in Table 3.4

Table 3.4. Hertizean contact stress

Moment Applied [Nm]	**Hertz Contact Stress [MPa]**
10	518
15	634.42
20	732.56
25	819
30	897.2
35	969.1
40	1036
45	1098.8
50	1158.3
55	1214.8
100	1638.1

3.3.3 Contact stress analysis and Surface fatigue life estimation by FEM

3.3.3.1 Contact stress analysis by FEM

There is no theoretical procedure to determine contact stress in between a pair of involute spur gears. AGMA has derived a near approximate procedure to determine the contact stresses by comparing them with Hertzian contact stress of two cylinders with parallel axis. In this chapter the contact stress in-between two involute gears is determined using a Finite Element Method.

There are many types of contact problems that may be encountered, including contact stress, dynamic impacts, metal forming, bolted joints, crash dynamics, assemblies of components with interference fits, etc. All of these contact problems, as well as other types of contact analysis, can be split into two general classes (ANSYS)

- Rigid to flexible bodies in contact.
- Flexible to flexible bodies in contact.

In rigid to flexible bodies in contact, one or more of the contacting surfaces are treated as being rigid material, which has a much higher stiffness relative to the deformable body it contacts. Many metal forming problems fall into this category.

Flexible-to-flexible is where both contacting bodies are deformable. Examples of a flexible-to-flexible analysis include gears in mesh, bolted joints, and interference fits.

In general, there are three basic types of contact model ing appl icati on as far as ANSYS use is concerned.

Point-to-point contact: the exact location of contact should be known beforehand. These types of contact problems usually only allow small amounts of relative sliding deformation between contact surfaces.

Point-to-surface contact: the exact location of the contacting area may not be known beforehand. These types of contact problems allow large amounts of deformation and relative sliding. Also, opposing meshes do not have to have the same discretization or a compatible mesh.

Surface-to-surface contact is typically used to model surface-to-surface contact applications of the rigid-to-flexible classification. Surface to surface contact is used in this work.

In order to handle contact problems in meshing gears with the finite element method, the stiffness relationship between the two contact areas is usually established through a spring that is placed between the two contacting areas. This can be achieved by inserting a contact element placed in between the two areas where contact occurs.

There are two methods of satisfying contact compatibility: (i) a penalty method, and (ii) a combined penalty plus a Lagrange multiplier method. The penalty method enforces approximate compatibility by means of contact stiffness. The combined penalty plus Lagrange multiplier approach satisfies compatibility to a user defined precision by the generation of additional contact forces that are referred to as Lagrange forces.

It is essential to prevent the two areas from passing through each other. This method of enforcing contact compatibility is called the penalty method. The penalty allows surface penetrations, which can be controlled by changing the penalty parameter of the combined normal contact stiffness. If the combined normal contact stiffness is too small, the surface penetration may be too large, which may cause unacceptable errors. Thus the stiffness must be big enough to keep the surface penetrations below a certain level. On the other hand, if the penalty parameter is too large, then the combined normal contact stiffness may produce severe numerical problems in the solution process or simply make a solution impossible to achieve. For most contact analyses of huge solid models, the value of the combined normal contact stiffness may be estimated [ANSYS] as, $k_n \approx fEh$

Where f is a factor that controls contact compatibility. This factor is usually be between 0.01 and 100, E is smallest value of young's modulus of the contacting materials ; h is the contact length

The contact stiffness is the penalty parameter, which is a real constant of the contact element. There are two kinds of contact stiffness, the combined normal contact stiffness and the combined tangential or sticking contact stiffness. The element is based on two stiffness values. They are the combined normal contact stiffness k_n and the combined tangential contact stiffness k_t.The combined normal contact stiffness k_n is used to penalize interpenetration between the two bodies, while the combined tangential contact stiffness k_t is used to approximate the sudden jump in the tangential force, as represented by the Coulomb friction when sliding is detected between two contacting nodes. However, serious convergence difficulties may exist during the vertical loading process and application of the tangential load often results in divergence. A detailed examination

of the model's nodal force during the vertical loading may indicate the problem. Not only are friction forces developing but they develop in random directions.

a. Program Controlled

This is the default setting. For this setting, the application selects the Pure Penalty property for contact between two rigid bodies and the Augmented Lagrange property for all other contact situations.

b. Pure Penalty

Basic contact formulation based on Penalty method.

c. Augmented Lagrange

Also a penalty based method. Compared to the Pure Penalty method, this method usually leads to better conditioning and is less sensitive to the magnitude of the contact stiffness coefficient. However, in some analyses, the Augmented Lagrange method may require additional iterations, especially if the deformed mesh becomes too distorted.

d. Multi Point Constraints (MPC)

Available for Bonded and for No Separation contact Types. Multipoint Constraint equations are created internally during the Mechanical APDL application solve to tie the bodies together. This can be helpful if truly linear contact is desired or to handle the nonzero mode issue for free vibration that can occur if a penalty function is used. Note that contact based results (such as pressure) will be zero.

e. Normal Lagrange

Enforces zero penetration when contact is closed making use of a Lagrange multiplier on the normal direction and a penalty method in the tangential direction. Normal Stiffness is not applicable for this setting. Normal Lagrange adds contact traction to the model as additional degrees of freedom and requires additional iterations to stabilize contact conditions. It often increases the computational cost compared to the Augmented Lagrange setting. The Iterative setting (under Solver Type) cannot be used with this method.

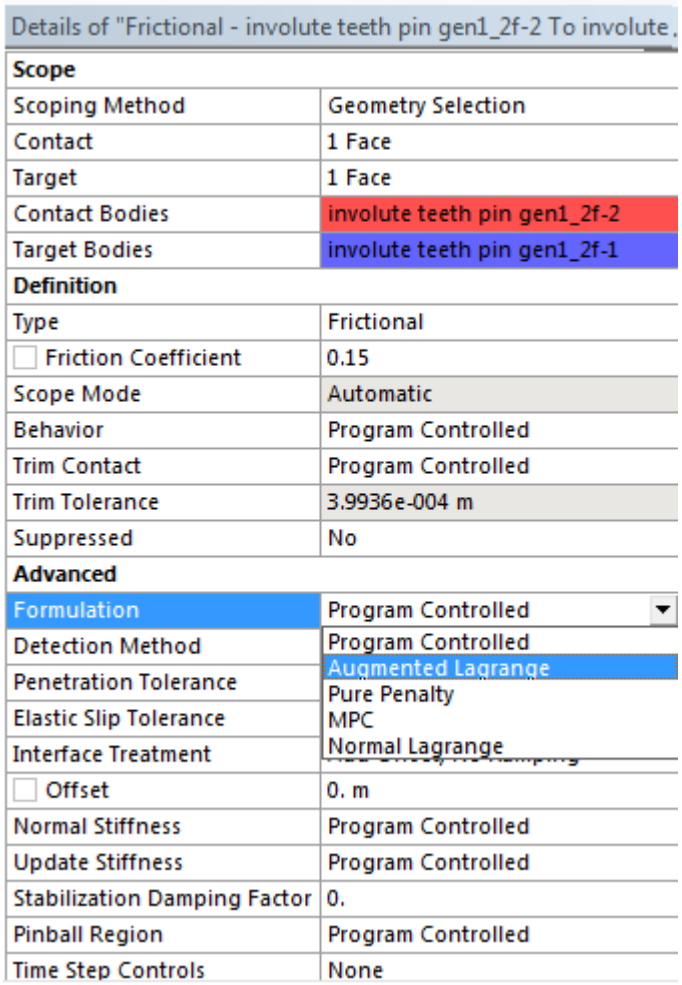

Figure 3.9 Contact formulation: Augmented Lagrange

3.3.3.2 Fatigue Life Estimation by FEM

The fatigue process of mechanical elements is a material characteristic and depends upon cyclic plasticity, local deformation, dislocation motion and formation of micro and macro-cracks and their propagation. Contact fatigue is extremely important for all engineering applications involving localized contacts such as gears, brakes, clutches, rolling bearings, wheels, rails, screws and riveted joints. The repeated rolling and/or sliding contact conditions cause permanent damage to the material due to accumulation of deformation.

A stress-time history is estimated for some part under investigation. Factors derived from geometry are then applied to turn this into a stress-time history. Traditionally these have been

taken from tables and graphs of stress concentration factors, which often do not cover the exact component geometry being used. Probably the most important role for FEA in this field is to replace and supplement these graphs. Comparing the stress-time history at the chosen critical point with this S-N curve allows a life estimate for the component to be made. In a variation of this method the S-N plots are obtained for whole components. Life estimates are then limited to that component, and a new test program should strictly follow even minor changes in its geometry. This is not a very economic procedure for modern development program and another major role for FEA is to avoid the need for it. The traditional and FEM procedures for fatigue life estimations are shown in Figure 3.10 and Figure 3.11 respectively.

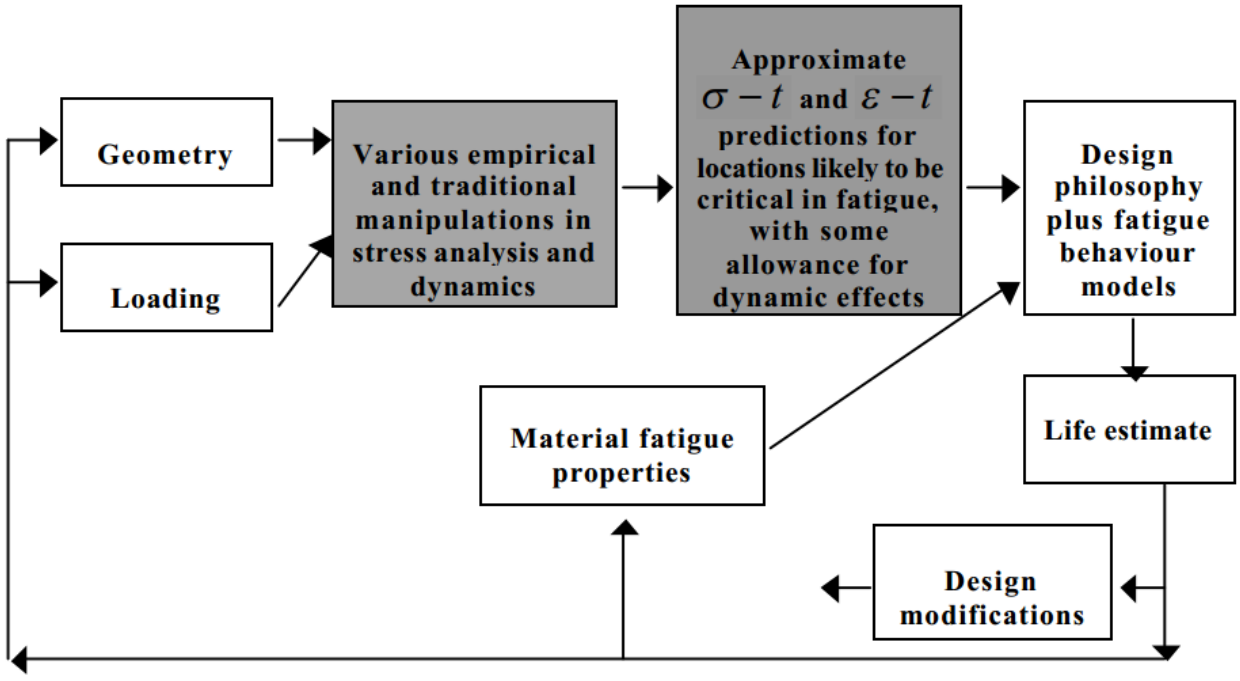

Figure 3.10 Traditional life estimation procedure [18]

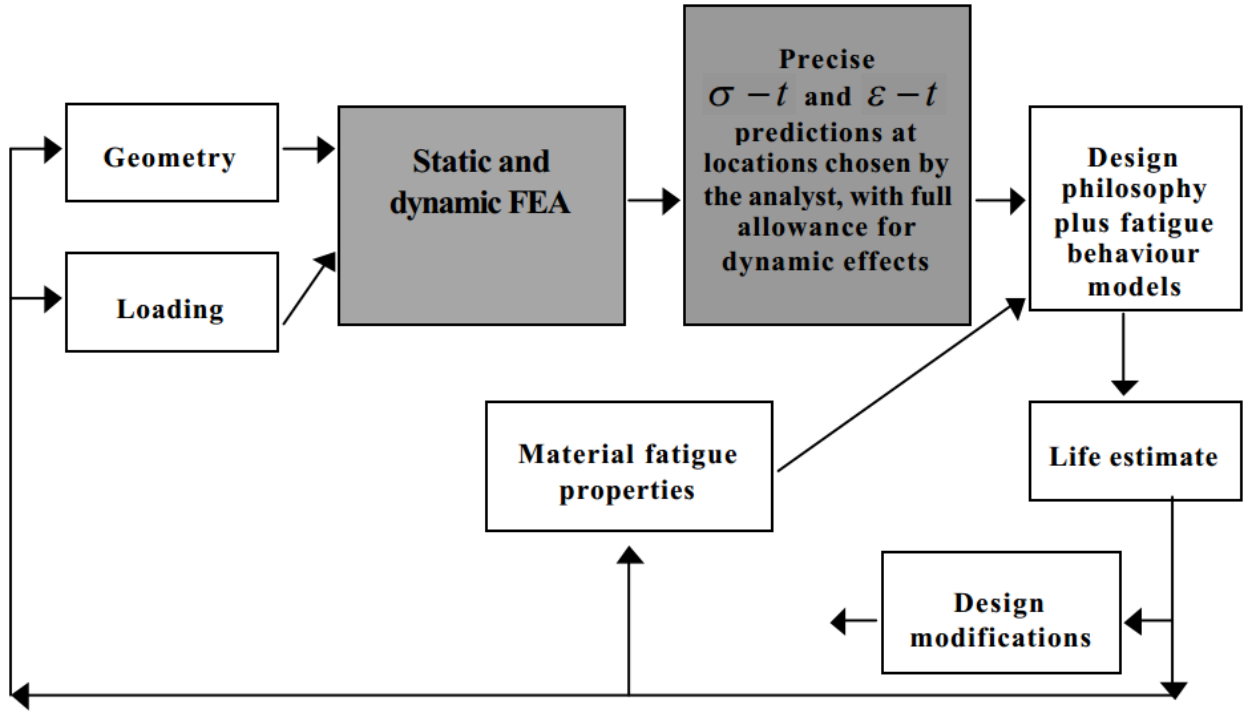

Figure 3.11 Fatigue life estimation scheme in FEM [18]

The Finite element analysis was done by using Solidworks 12 for modeling of pair of involute spur gear and assembling them and Ansys Workbench 14.5 was used for analysis of contact stress and surface fatigue life estimation. The following steps were used for the aforementioned modeling and analysis:

i The involute spur gear profile is generated using equations (3.3.1) in SOLIDWORKS PREMIUM 2012. Then the 2D model for pinion is generated as shown in Figure 3.12 a and b.

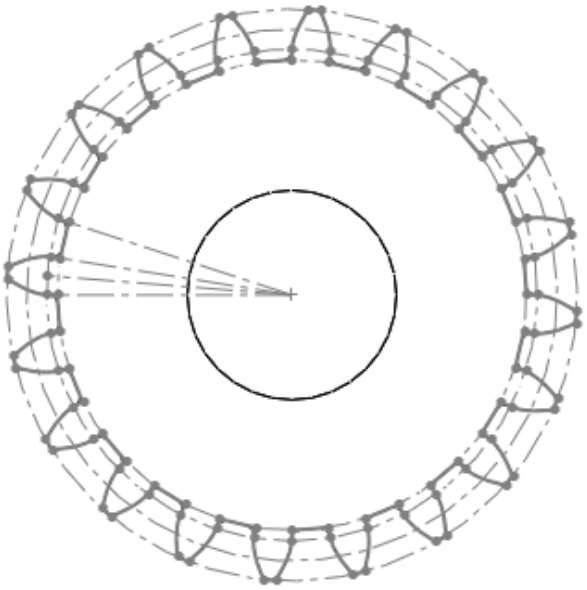

a)

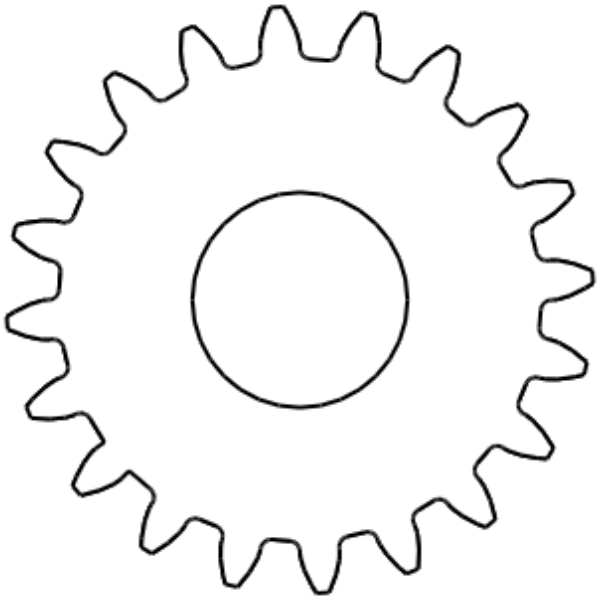

b)

Figure 3.12 a) Involute spur gear genaration b) 2D Involute spur gear

ii The 2D involute profile generated in step i is then extruded by taking a given face width as a length of extrusion. It is shown in Figure 3.13.

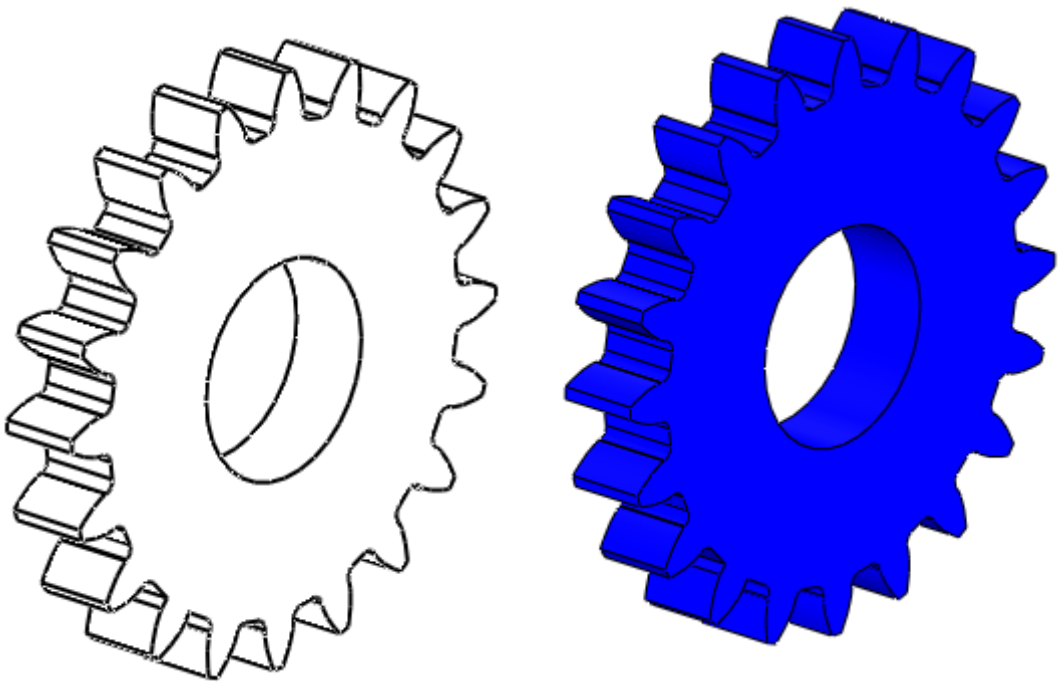

Figure 3.13 3D Involute spur gear model

iii Steps i and ii were repeated to generate the gear (for ease of analysis the dimensions of the pinion and gear were assumed to be the same) and then the pinion and gear were assembled in the proper orientation. (See Figure 3.14)

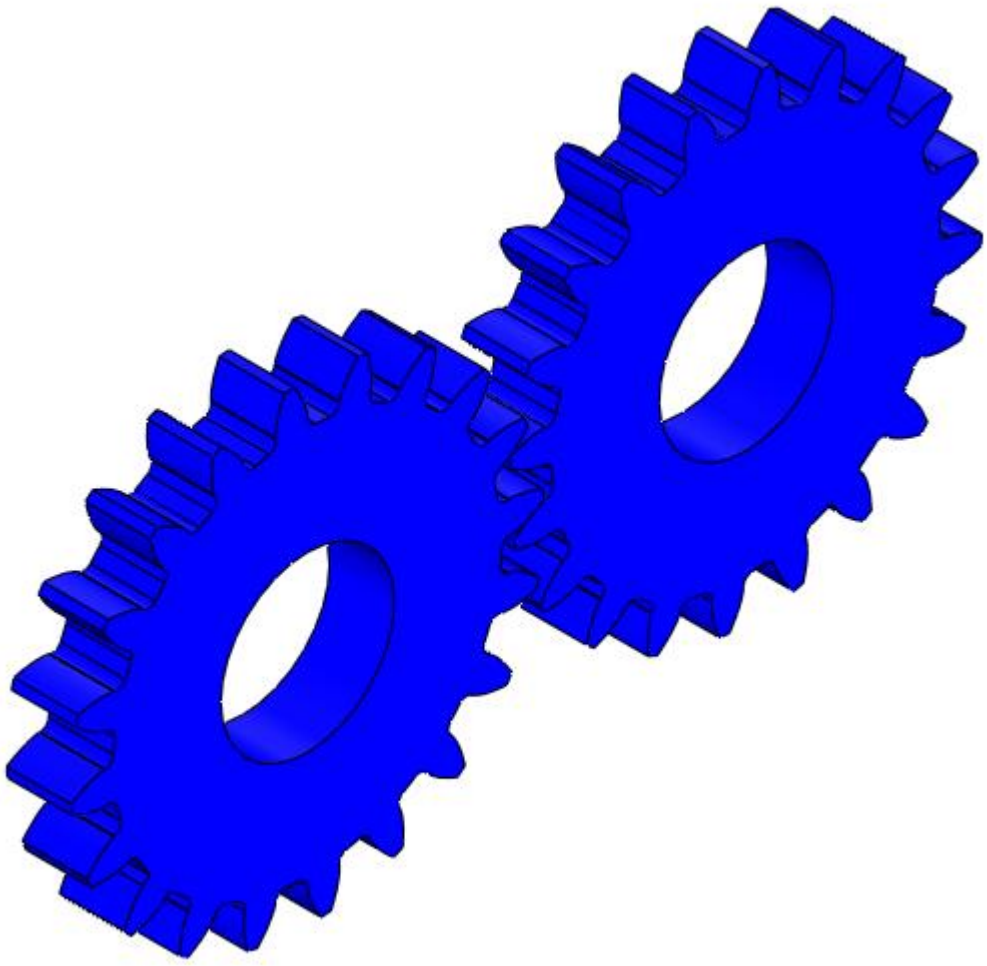

Figure 3.14 Meshed model of pair of Involute spur gear

iv Importing the assembled model in to ANSYS WORKBENCH 14.5, the structural analysis was performed. To get the contact stresses the contact wizard is used in ANSYS Workbench. The contact algorithm in ANSYS Workbench computer program requires definition of contacting surface. To define a contact pair completely, contact and target element have to be referred to same characteristic parameters. The contact element CONTA174 and target 170 are used in the present analysis. Then, augmented Lagrangian method contact algorithm, with frictional contact (coefficient of friction = 0.15) is used.

v After the proper model is finished, the computational mesh that is used as a basis of solution procedure should be generated. The mesh consists of discrete elements located throughout the computational domain. A good computational mesh is an essential ingredient for a successful and accurate solution. If the overall mesh is too coarse, the resulting solution may be inaccurate. If the overall mesh is too fine, the computational cost may become prohibitive. In summary, the cost and accuracy of the solution are directly dependent on the quality of the mesh. So the mesh was fine near the contact and course away from the contact surfaces as it is seen in Figure .

vi Ansys has the capability of increasing elements at contact elements. The density of the elements is given in terms of levels from 1 to 3. Value of one being minimal refinement at the specified location and 3 provides maximum refinement. The elements are generated in a haphazard manner and even violate shape limits. Figure 3.15 shows the application of refinement

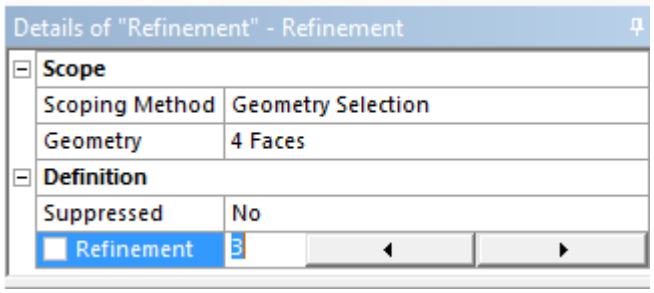

Figure 3.15 Refiniment of contact area

vii When used with assembly meshing, contact sizing provides a method for closing leaks discovered during meshing. Typically, leakage occurs if any contact is larger than 1/10 of the local minimum size. If a leak is discovered during meshing and the gap is up to 1/3 of the local mesh size, you can close the gap at the location of contact by using a two-step process. First, scope a new contact to the existing Find Contacts list by picking all of the

faces on one side and all of the faces (or edges) on the other side of the leak. Second, scope a contact sizing control to this new contact.

viii For assembly meshing, the default Element Size used by contact sizing controls is minimum_size/5, where minimum size is the value of Min Size or Proximity Min Size, whichever is smaller. This Element Size is appropriate for the vast majority of cases. However, you may need to adjust the value of Element Size in these situations:

ix If hard sizing that is smaller than Min Size/Proximity Min Size is applied in the vicinity of the contact region, you may need to reduce the Element Size used by contact.

x If local sizing that is significantly larger than Min Size/Proximity Min Size is applied in the vicinity of the contact region, you may need to increase the Element Size used by contact.

xi Each face-edge contact region in a contact sizing control consists of one or more faces and one or more edges. That is, in some cases a contact region may consist of one face to one edge in contact, while in others it may consist of many faces to many edges.

xii Use care in specifying Element Size for contact sizing. A value that is too large may lead to inaccurate geometry, while a value that is too small may fail to close the leak. A good guideline is to specify an Element Size that is 1/5 of the local element size.In some cases the gap at the location of contact is closed but the mesh in that location will not be well resolved. This occurs because there are no features to be captured at the location of the gap, which in turn causes the edges to become jagged. The contact size taken for this research is 0.0004 m and the application of contact sizing in Ansys Workbench 14.5 is shown in Figure 3.16

Details of "Contact Sizing" - Contact Sizing

Scope	
Contact Region	Frictional - involute teeth pin gen1_2f-2 To involu...
Definition	
Suppressed	No
Type	Element Size
Element Size	4.e-004 m

Figure 3.16 Contact sizing application in Ansys Workbench.

a)

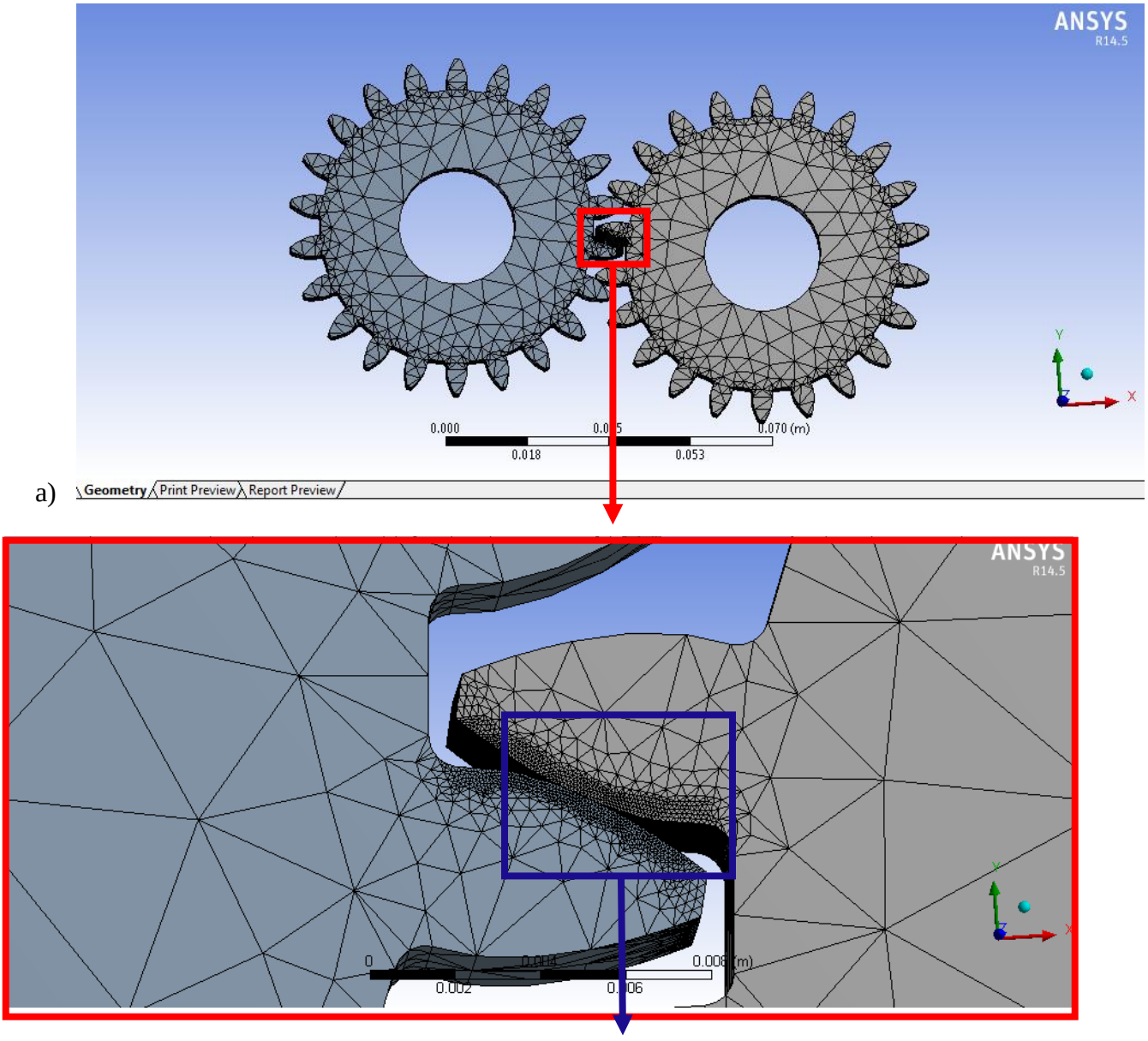

c) 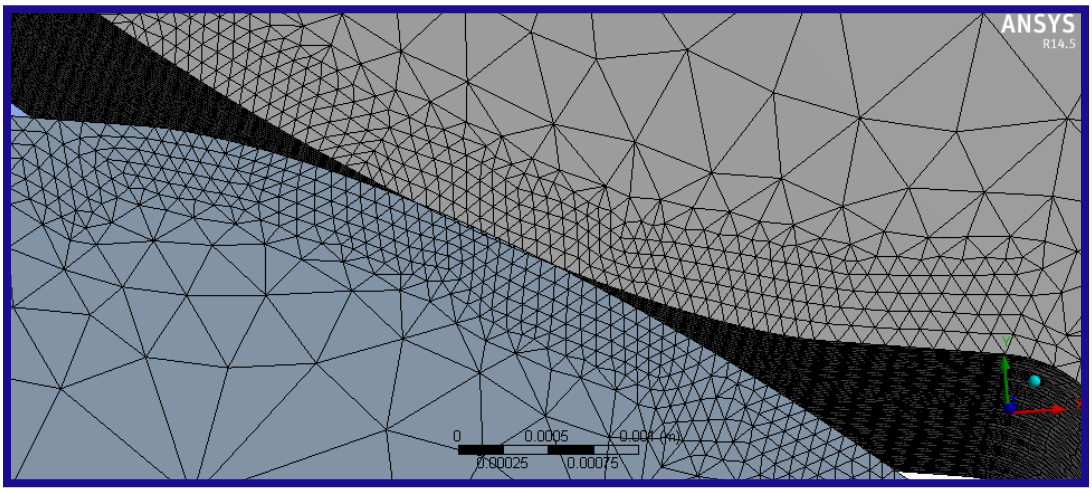

Figure 3.17 Fine mesh near the contact area a), b) and c) with different magnification

i The boundary conditions for the pinion and gear were taken as follows: the inner race of the pinion given frictionless support and the inner race of the gear is given a fixed support as shown in Figure 3.18. Displacement boundary condition applied as it is seen in Figure 3.19. And finally moment was applied at the pinion as it is seen in Figure 3.20. The details of moment application is shown in Figure 3.21 and all boundary conditioned are shown in Figure 3.22.

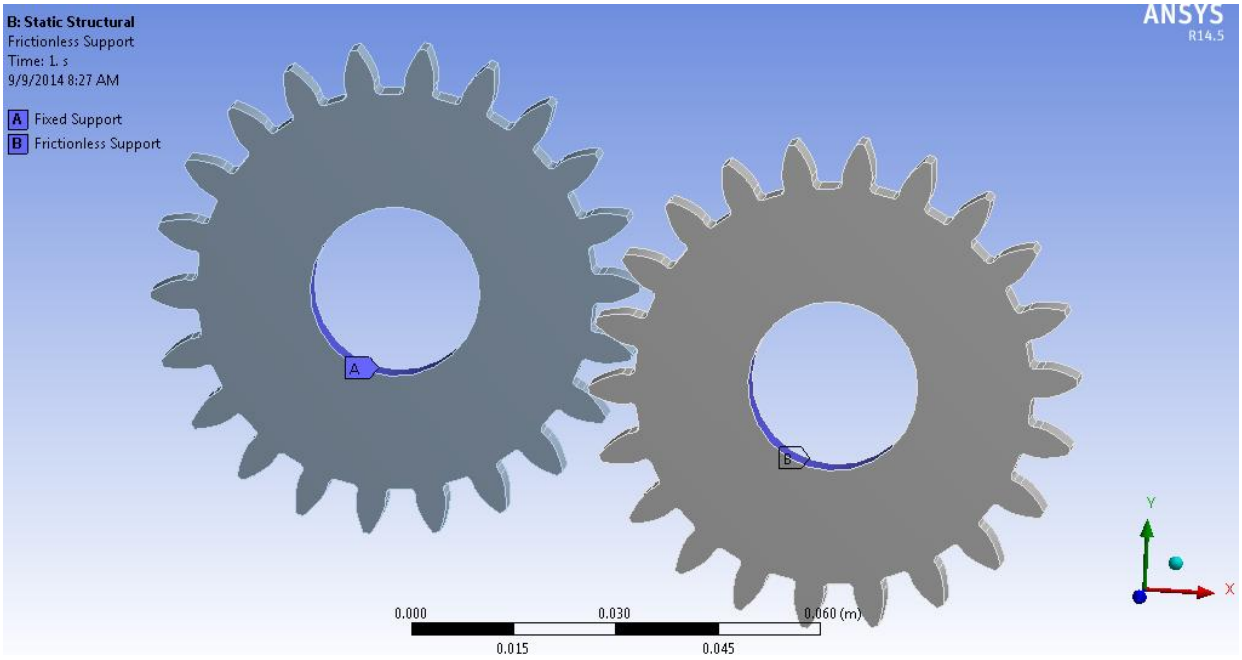

Figure 3.18. Support Boundary Conditions

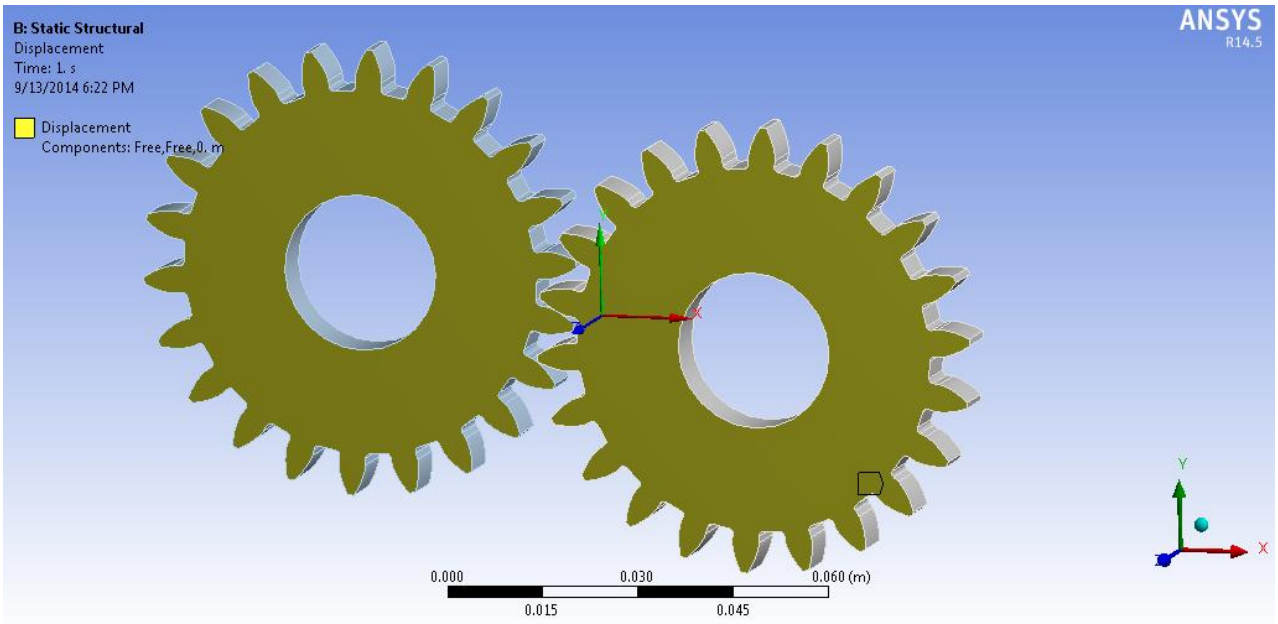

Figure 3.19. Displacement Boundary Conditions

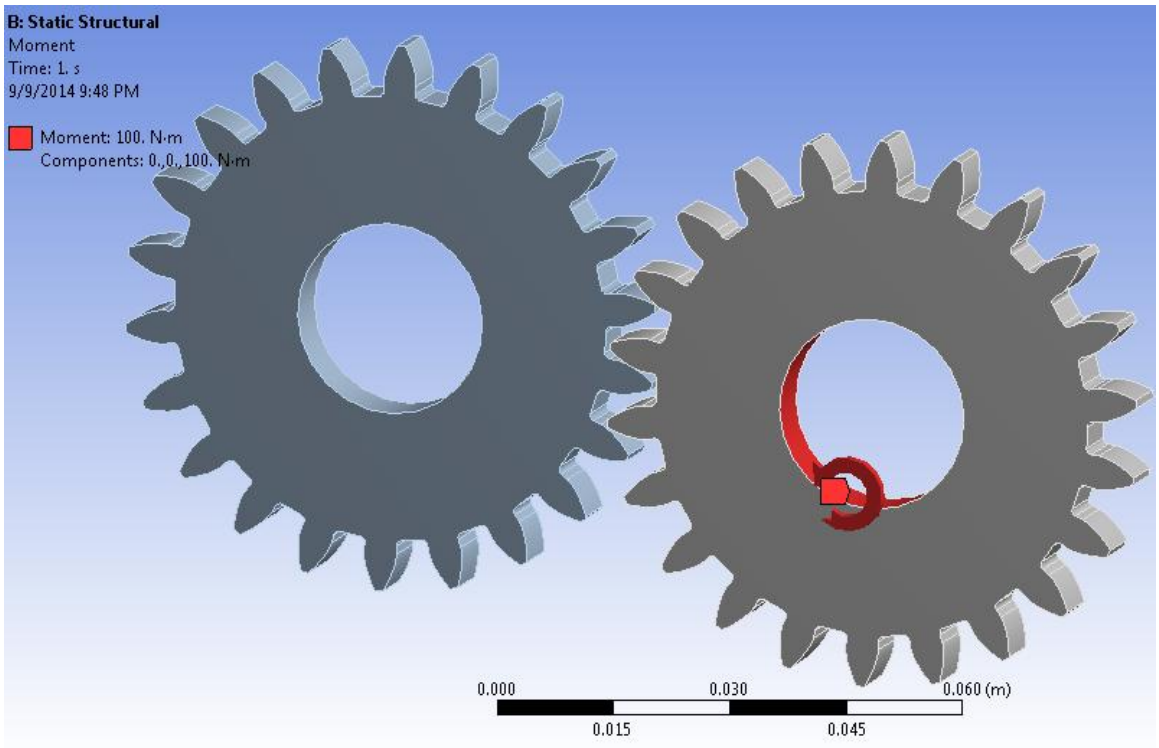

Figure 3.20. Moment application

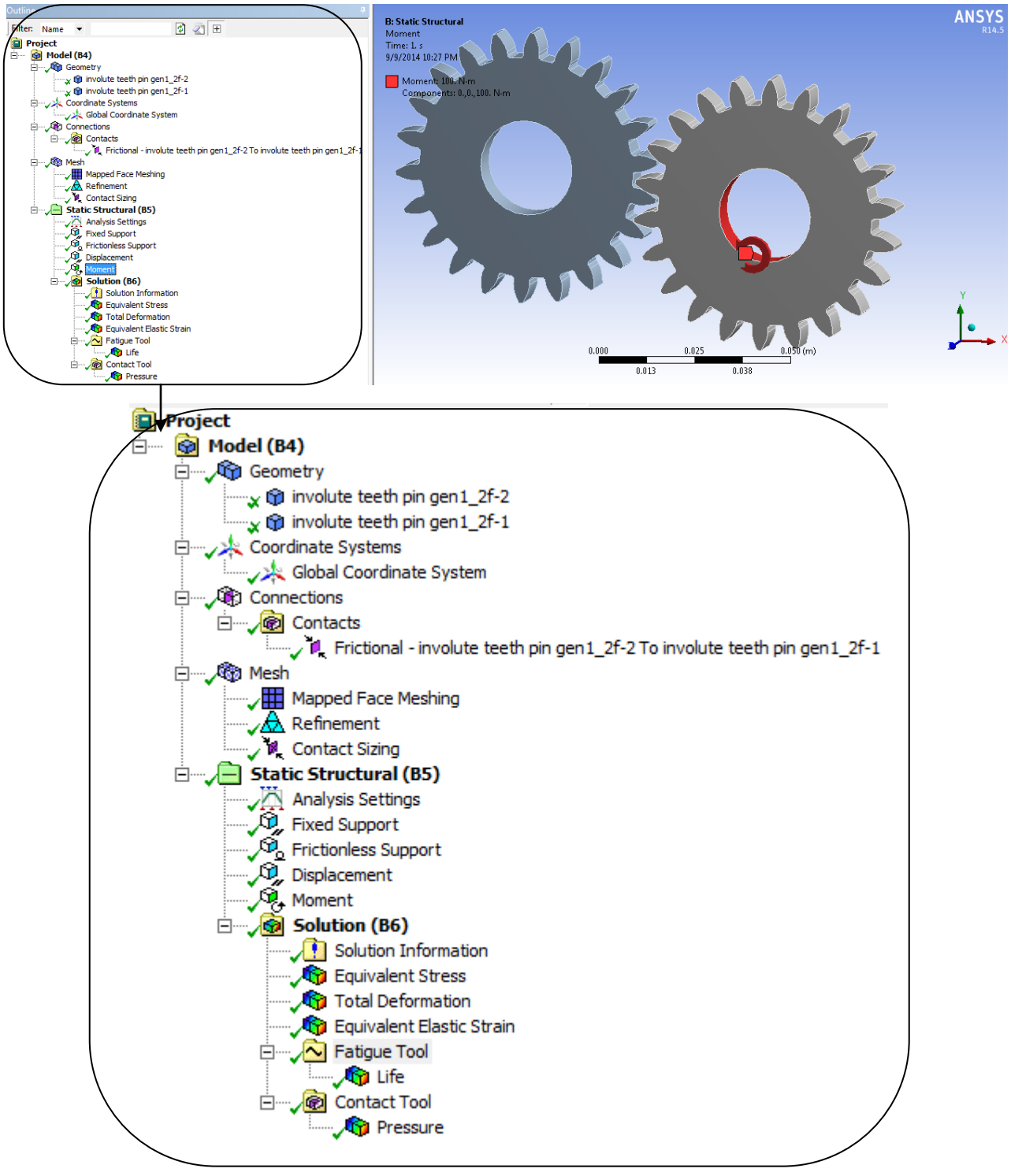

Figure 3.21. Details of Moment application

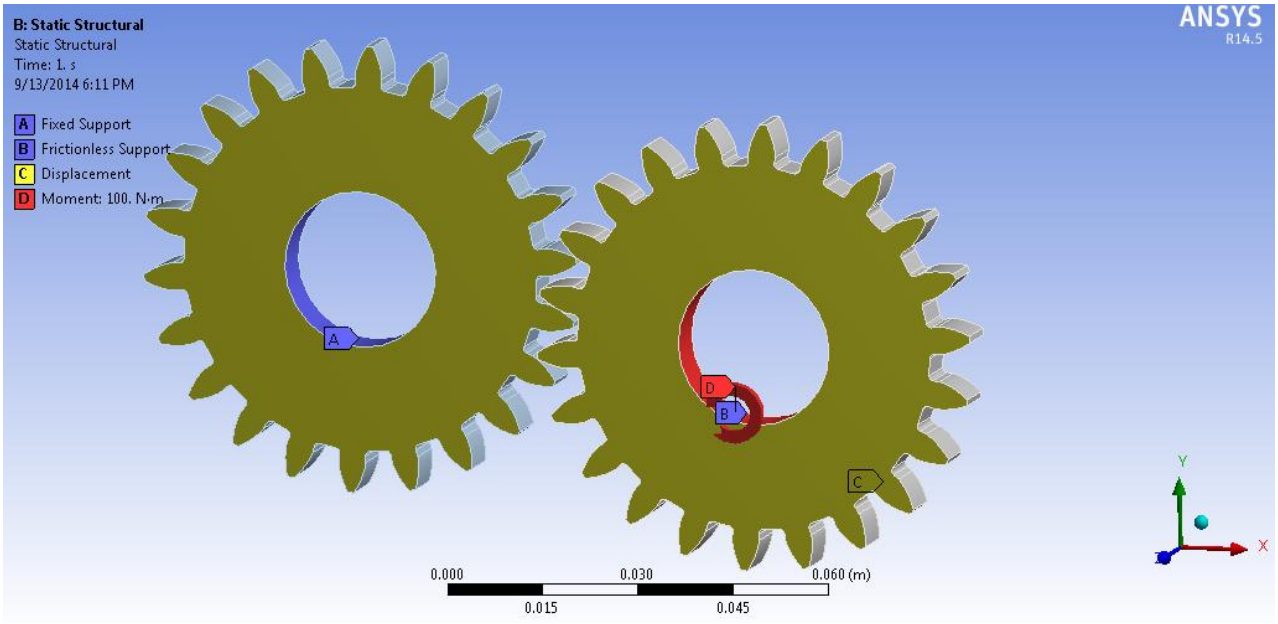

Figure 3.22 All boundary conditions applied on the model

ii After setting of boundary conditions for gear and pinion initiating the solver to compute the required results.

Chapter Four

4. Result and Discussion

4.1 Contact stress analysis

From practical point of view Finite Element Method is preferable for contact stress analysis of involute spur gear [21]. The contact stress develped in the area of contact of the pinion and gear was calculated analyticall by using Hertz stress equation and by Finite Element Method by using Ansysworkbench releas 14.5.

The number of mesh determines the accuracy of the result and computational time when we increase the number of mesh computational time will be high and needs high performance computer when we decrease the number of mesh elements the accuracy will be less. Thus to alleviate those problems the usual trend is to use fine mesh in the area of interest (in this case the contact area) and course mesh away from the contact region.

The contact stress was found for different loading which ranges from 10Nm to 100Nm from Hertz equation and from finite element method is shown in Table 4.1. As it is shown on the same table the error between analytacal and FEM values decreases with increasing loading condition and even for smaller loads the error is tolerable. The contact stress distribution is shown in Figure 4.1. Figure 4.2 show the effect of contact stress on the over all stress in the gear pair because the maximum equivalent stress is in the contact area where contact stress is maximum.

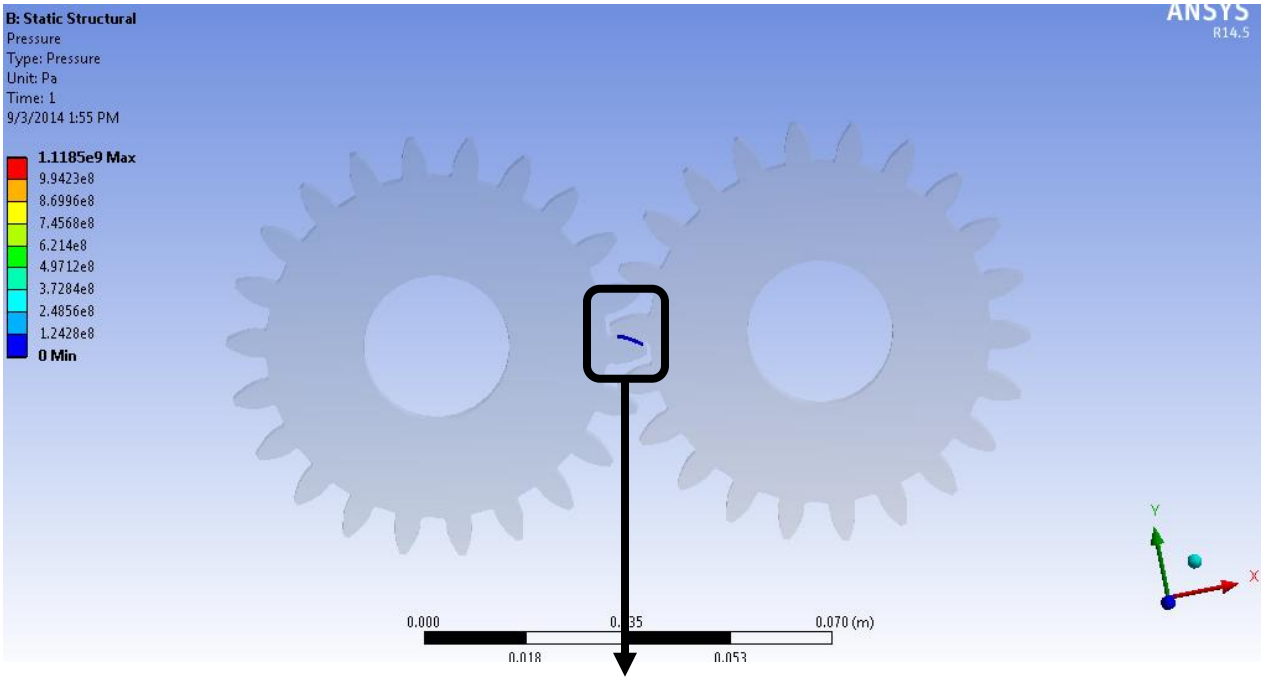
B: Static Structural
Pressure
Type: Pressure
Unit: Pa
Time: 1
9/3/2014 1:55 PM
1.1185e9 Max
9.9423e8
8.6996e8
7.4568e8
6.214e8
4.9712e8
3.7284e8
2.4856e8
1.2428e8
0 Min
ANSYS
R14.5
0.000
0.070 (m)
0.018
0.053

(a)

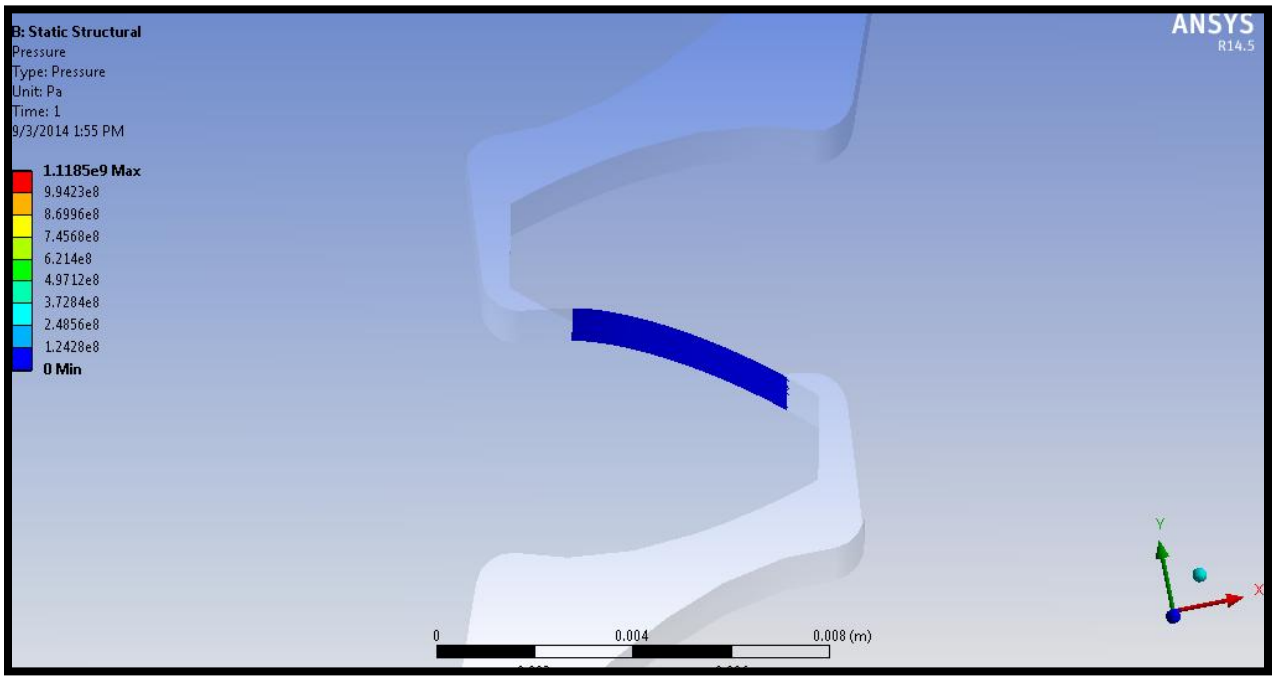
B: Static Structural
Pressure
Type: Pressure
Unit: Pa
Time: 1
9/3/2014 1:55 PM
1.1185e9 Max
9.9423e8
8.6996e8
7.4568e8
6.214e8
4.9712e8
3.7284e8
2.4856e8
1.2428e8
0 Min
ANSYS
R14.5
0
0.004
0.008 (m)

(b)

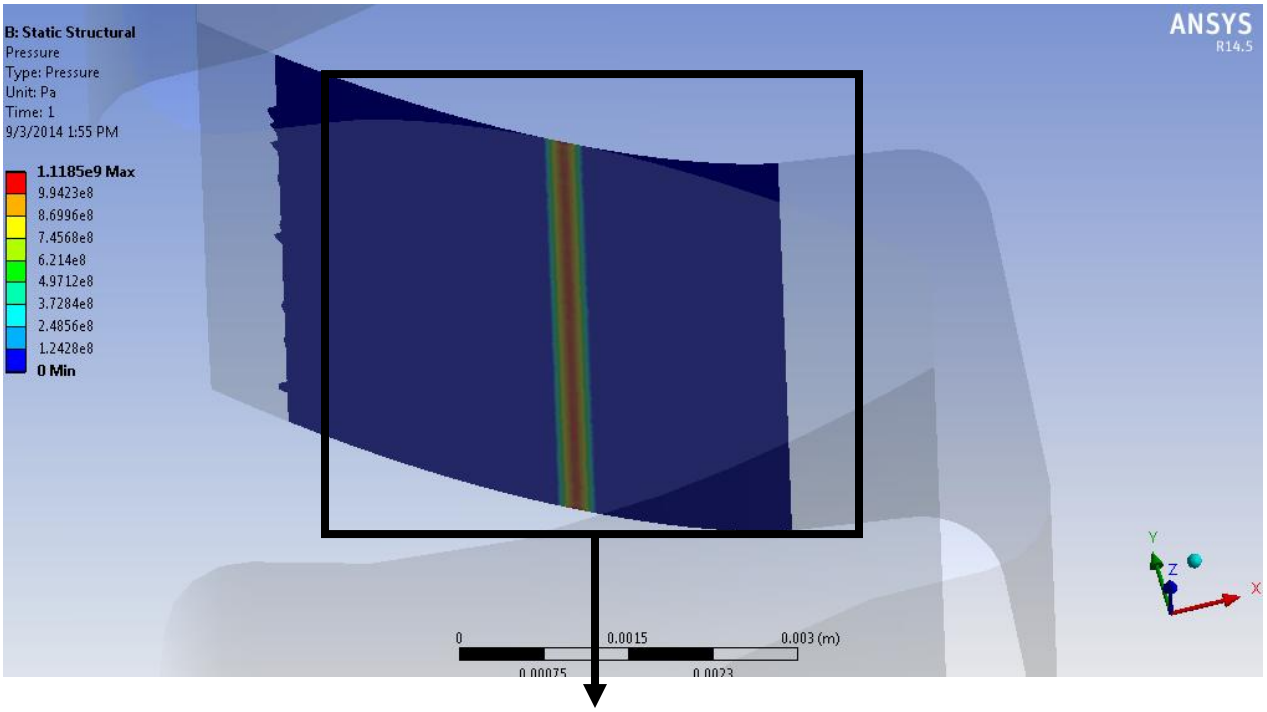

(c)

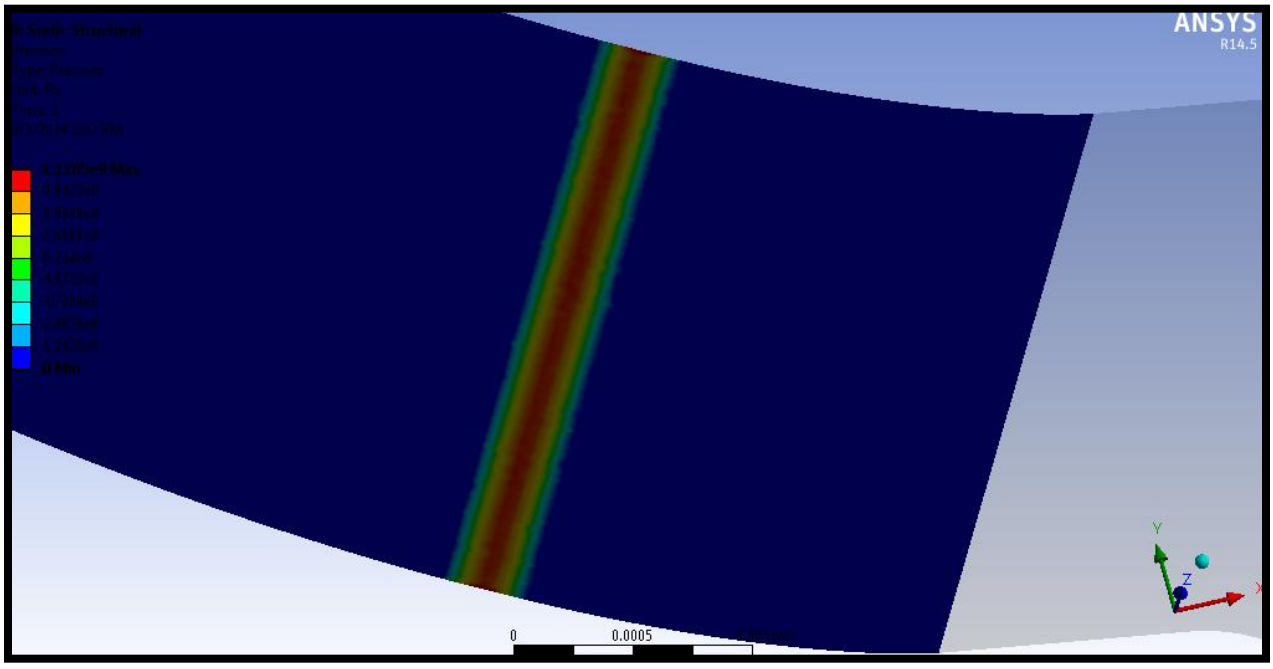

(d)

Figure 4.1 Cntact stress by FEM (a) contact area b) Magnified contact area c) contact stress for 50Nm load d) Magnified contact stress distribution.

Table 4.1. Comparison of contact stress by analytical and FEM methods

Contact sizing =0.0004m ;Friction coefficient=0.15			
Moment Applied [Nm]	**Contact Stress (Ansys Workbench) [MPa]**	**Hertz Contact Stress [MPa]**	**Error (%)**
10	486.38	518	6.03
15	596.22	634.42	6.02
20	694.31	732.56	5.22
25	778.5	819	4.95
30	853.98	897.2	4.8
35	925.89	969.1	4.46
40	992.78	1036	4.17
45	1056.5	1098.8	3.85
50	1118.5	1158.3	3.48
55	1177.7	1214.8	3.05
100	1662.6	1638.1	1.496

Since there is no previous experimental work done with the same parameter the FEM result is compared with Hertizean contact stress. The Hertizean contact stress calculated for the moments 10,15,20,25,30,35,40,45,50,55,100Nm are calculated and then for those elements the maximum contact pressures are found from FEM by Ansysworkbench 14.5. As seen in Table 4.1 the error for 100Nm is 1.496 and it would be less for higher moment. The contact stress from Hertizean stress and from Ansysworkbench is plotted in Figure 4.2.The error versus applied moment is plotted as shown in Figure 4.3 as it is seen in the figure the error decreases when the load increases.

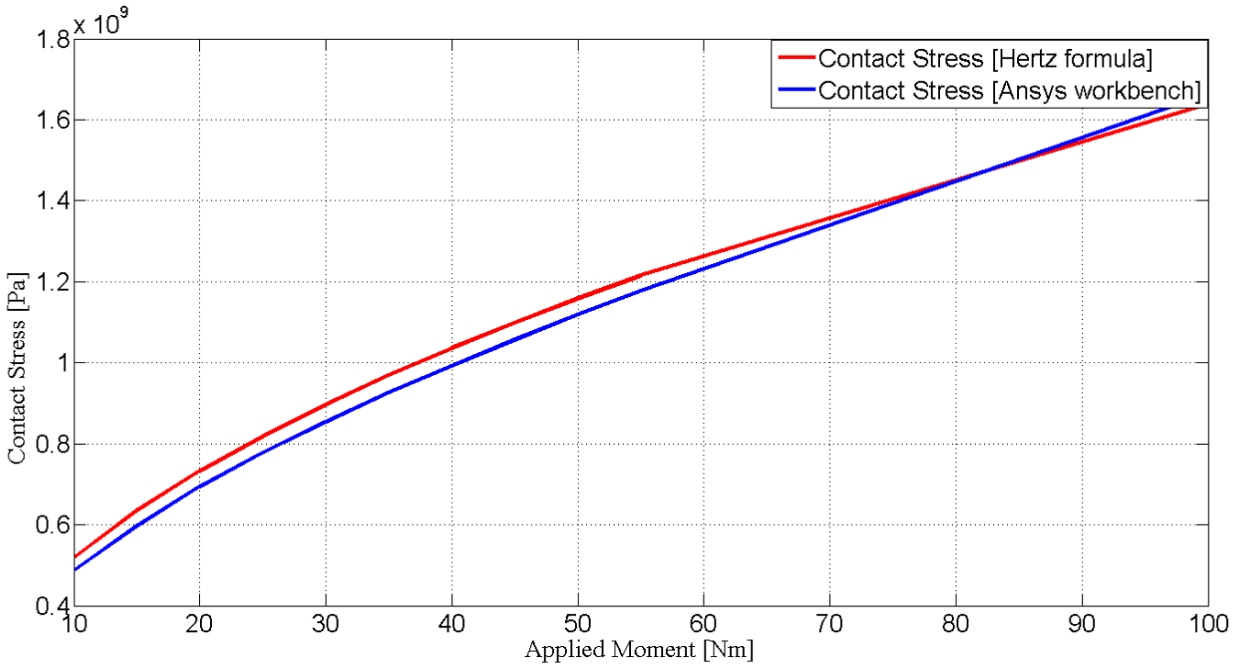

Figure 4.2 Contact stress by Hertz formulae and by FEM

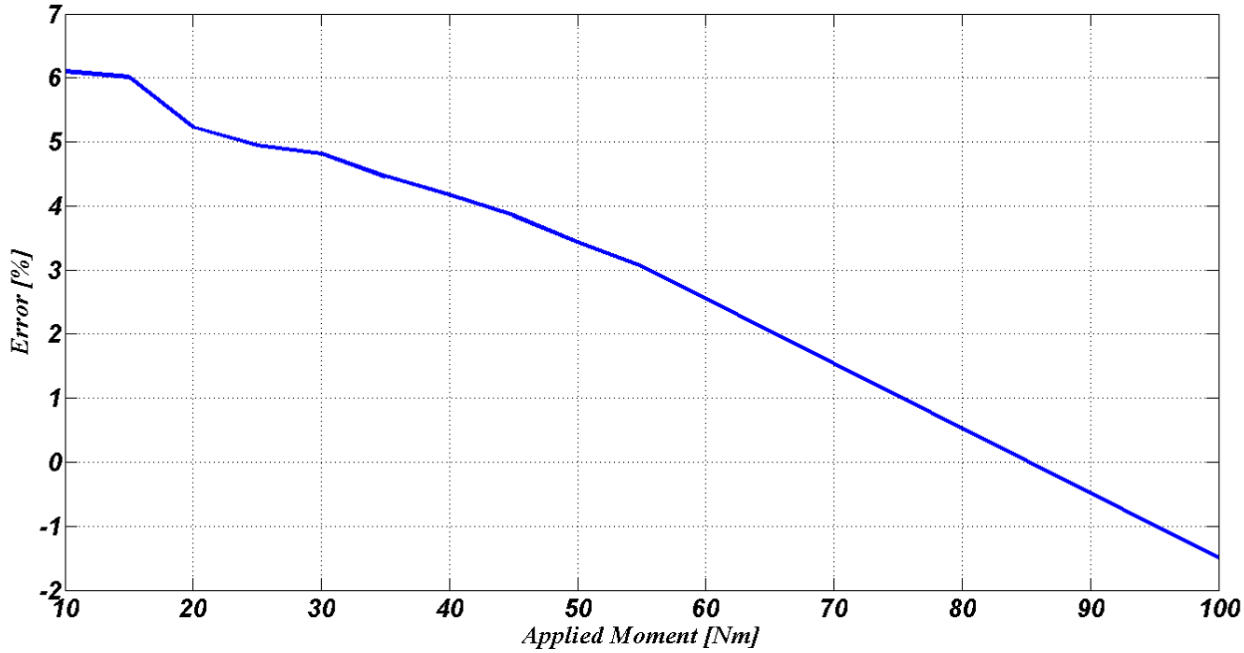

Figure 4.3. Percentage deviation of FEM from analytical method

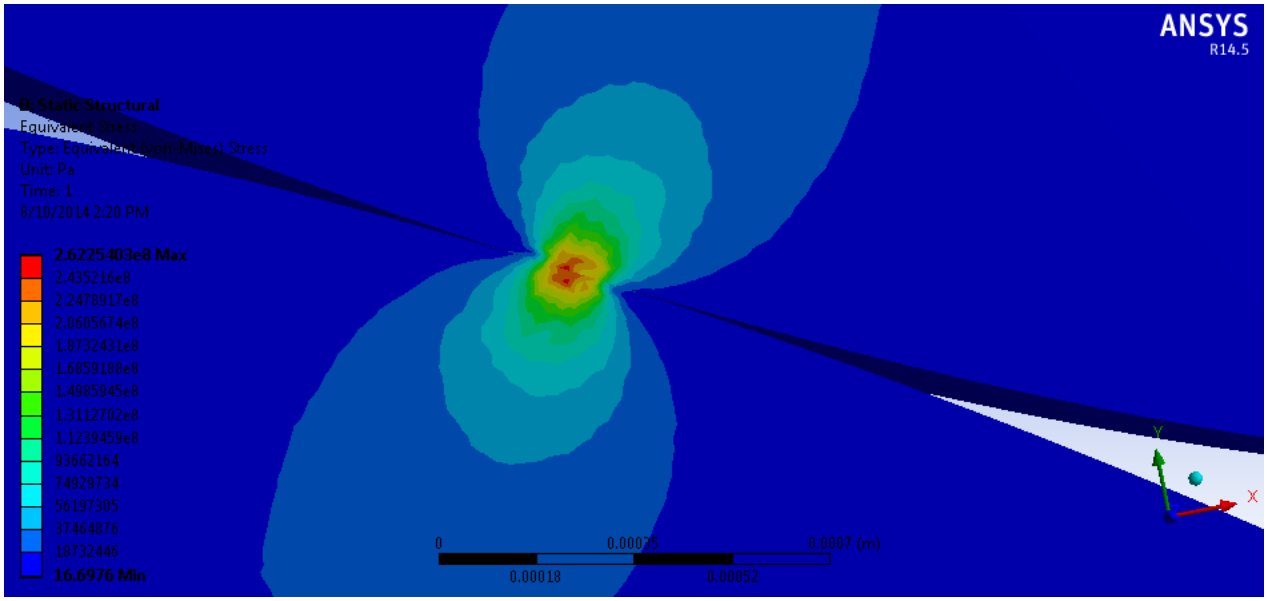

Figure 4.4 Equivalent (Von mises) stress

Table 4.2. Contact stress for different coefficient of friction

Friction coefficient	Contact stress [MPa]
0.01	1094
0.05	1101
0.1	1110.01
0.15	1118.5
0.2	1127.6

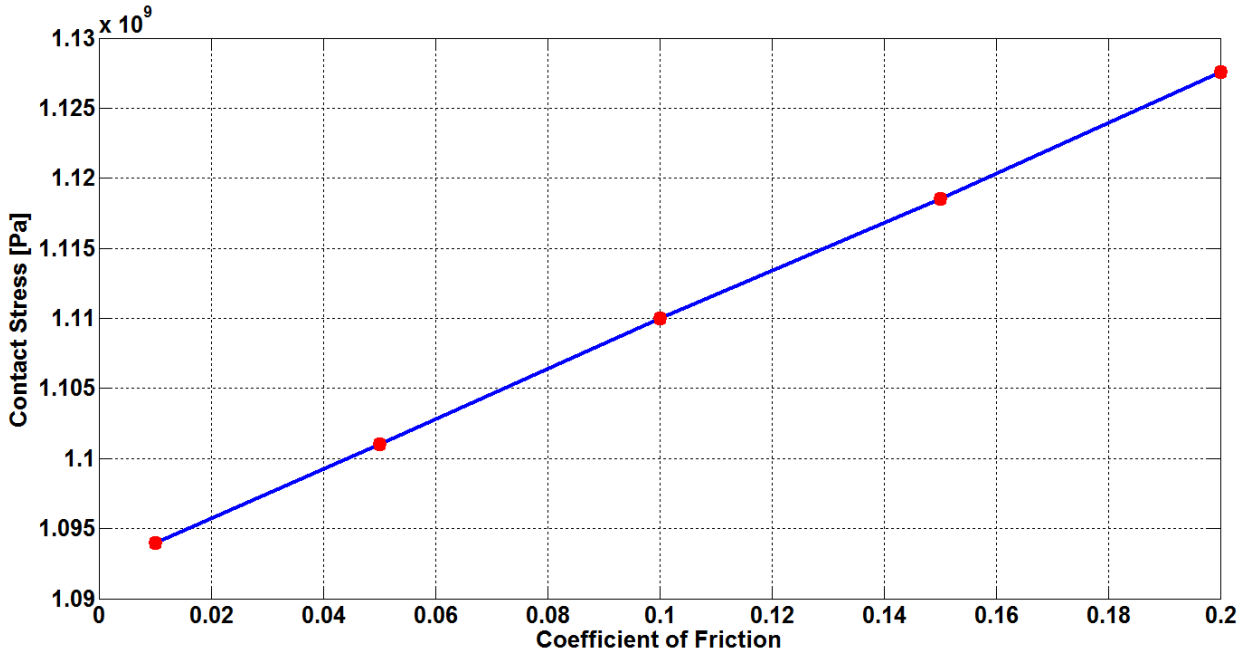

Figure 4.5 Contact Stress for different coefficient of friction

The variation of contact stress with coefficient of friction is shown in Figure 4.5 as it is seen in the figure contact stress increases with increasing coefficient of friction. From this we can infer that minimizing friction by using improved surface finish; applying lubrication in the area of contact and/or by using a better material will minimize the contact stress hence reduce wear which result in better surface fatigue life.

The contact stress from Heartizean stress and maximum contact stress by FEM using ansys workbench 14.5 for the materials : structural steel, chromium molibdinum , Grey cast iron GG20, Grey cast iron GG25 and Grey cast iron GG30 is shown in Table 4.3

The values of contact stress by Hertizean stress and contact stress by FEM , shown in Table 4.3, is dependent on the material property.

Table 4.3. Contact stress by FEM and Hertizean formula for five different materials

Material	**Ansys Maximum Contact stress[MPa] when torque applied =100Nm**	**Hertz Maximum Contact Stress [MPa] when torque applied =100Nm**
Chromium Molybdenum	1679.8	1662.5
Structural steel	1662.6	1638.1
Grey cast iron GG20	1151.7	1088.6
Gray cast iron GG25	1110.7	1169.4
Gray cast iron GG30	1113	1213.1

The graph of contact stress by Hertizean theory and by FEM for different Material at applied moment of 100Nm is plotted using Matlab release 10b shown in Figure 4.6.

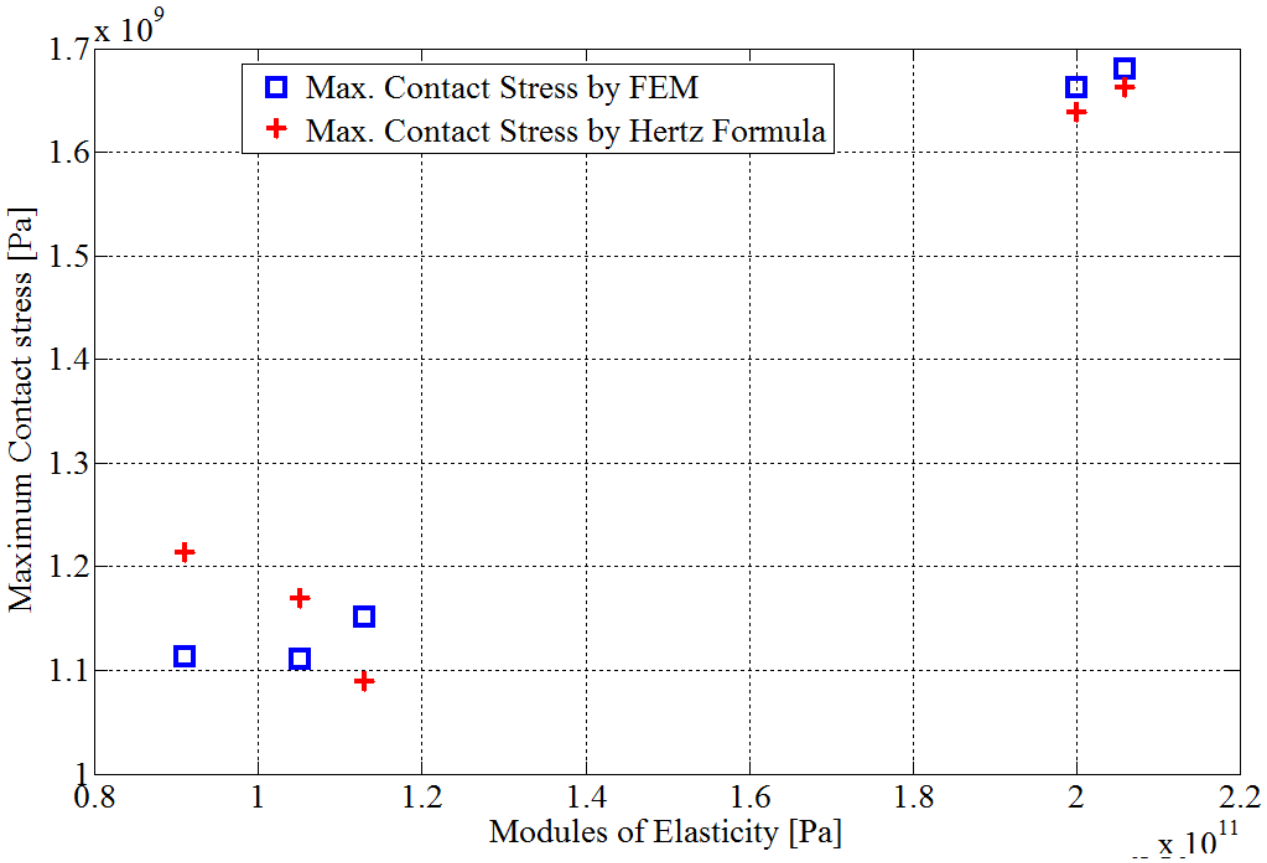

Figure 4.6 Contact Stress for materials with different Modulus of elasticity

4.2 Surface Fatigue Life Estimation by FEM

4.2.1 Introduction

Because fatigue cracks initiate predominantly at the free surface of a material, the surface condition of a test sample becomes critical. The surface condition can be characterized by considering two factors: (1) notch-like surface irregularities or roughness and (2) residual stress in the surface layer. Irregularities along the surface act as stress concentrations and result in crack initiation at the surface. Figure 4.7 is an empirical chart used to determine the surface finishing modifying factor for steels when measurement of the surface roughness is known.

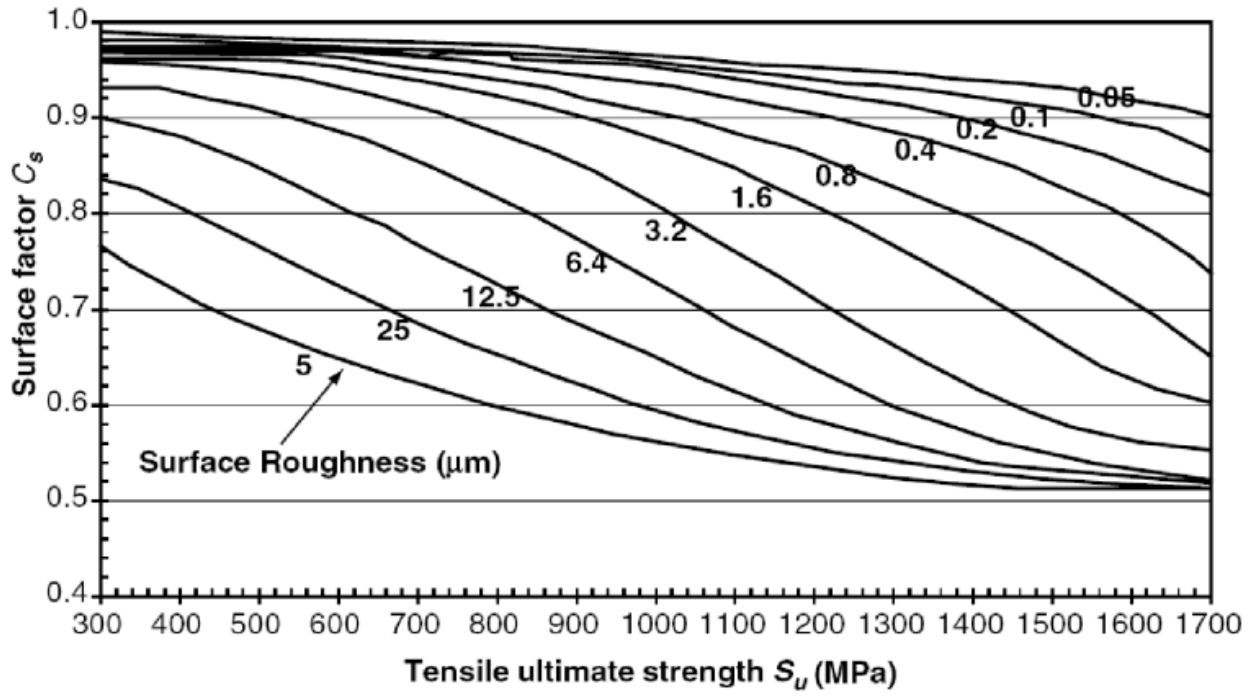

Figure 4.7. Qualitative description of C_s surface finish factor. Adapted from Johnson (1973) as it is cited in [19].

Surface treatments are usually used to induce residual surface stresses. Some operations such as chemical process (decarburization, carburization, and nitriding), electroplating, and thermal processing can alter the physical properties of the surface layer. And induce tensile residual stress. These tensile stresses result in fatigue strength reduction. Carburization and nitriding process force carbon and nitrogen in to the surface layer and strengthen the surface layer and produce compressive residual stress these compressive residual stress increase the fatigue strength of materials.

Mechanical processes can introduce residual stresses into a material. For example, tensile stress can be generated from machining and compressive residual stresses may be introduced in a material by peening and cold working processing. Figure 4.8 is used to estimate the surface modifying factors based on manufacturing process for steels. In general, surface finish is more critical for high-strength steel and at high-cycle fatigue lives where crack initiation dominates the

fatigue life. At short lives where crack propagation dominates the fatigue life, the effect of surface finish on fatigue strength is minimal.

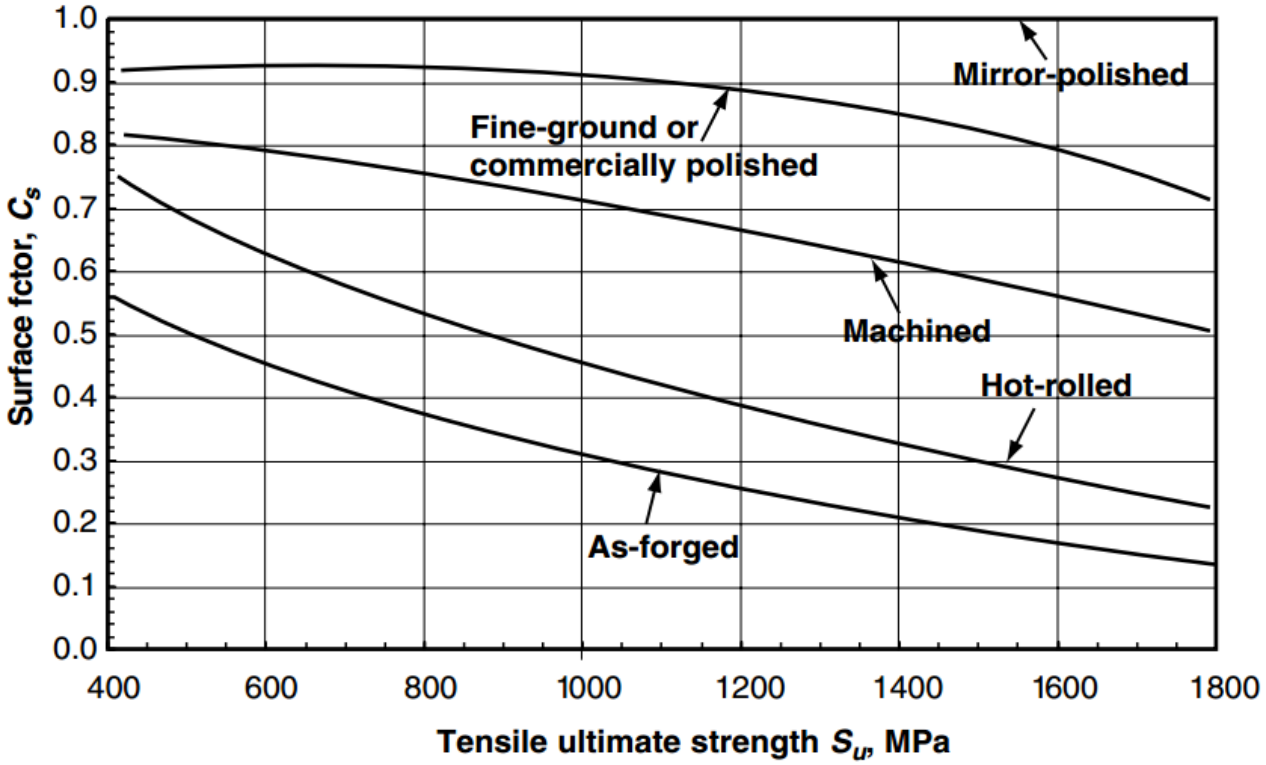

Figure 4.8. Qualitative description of C_s surface finish factor. Adapted from Juvinall and Marshek (2000) as it is cited in [19].

4.2.2 Surface fatigue Life Estimation by Ansysworkbench 14.5.

Fatigue is the phenomenon in which a repetitively loaded structure fractures at a load level less than its ultimate static strength. For instance, a steel bar might successfully resist a single static application of a 300 kN tensile load, but might fail after 1,000,000 repetitions of a 200 kN load. The primary factors that contribute to fatigue failures include:

- Number of load cycles experienced
- Range of stress experienced in each load cycle
- Mean stress experienced in each load cycle
- Presence of local stress concentrations

A formal fatigue evaluation accounts for each of these factors as it calculates how "used up" a certain component will become during its anticipated life cycle.

Of the four aforementioned primary factors presence of local stress concentration is relatively difficult to quantify and many factors influences its value of these surface roughness and manufacturing method are main factors and their qualitative description is shown in Figure 4.7 and Figure 4.8 respectively. These influencing factors are not directly available in ansys workbench however there is a factor called fatigue strength factor (Kf). By keeping all other stress concentration factors constant the fatigue strength factor is set for different manufacturing methods is shown in Table 4.4.

Table 4.4. Fatigue strength factor for different manufacturing processes

Manufacturing process	Surface roughness(μm)	Fatigue strength factor(Kf)
Mirror polished	0.05	1
Fine-ground	12.5	0.9
Machined	25	0.8
Hot rolled	50	0.7

The fatigue life of the pair of involute spur gear is then estimated by FEM using Ansys Workbench 14.5. For chromium Molybdenum Fatigue life of the gear under different loading for different fatigue strength factor is shown in Table 6.2.3.And the FEM analysis in Ansys workbench 14.5 is shown in Figure 4.9.

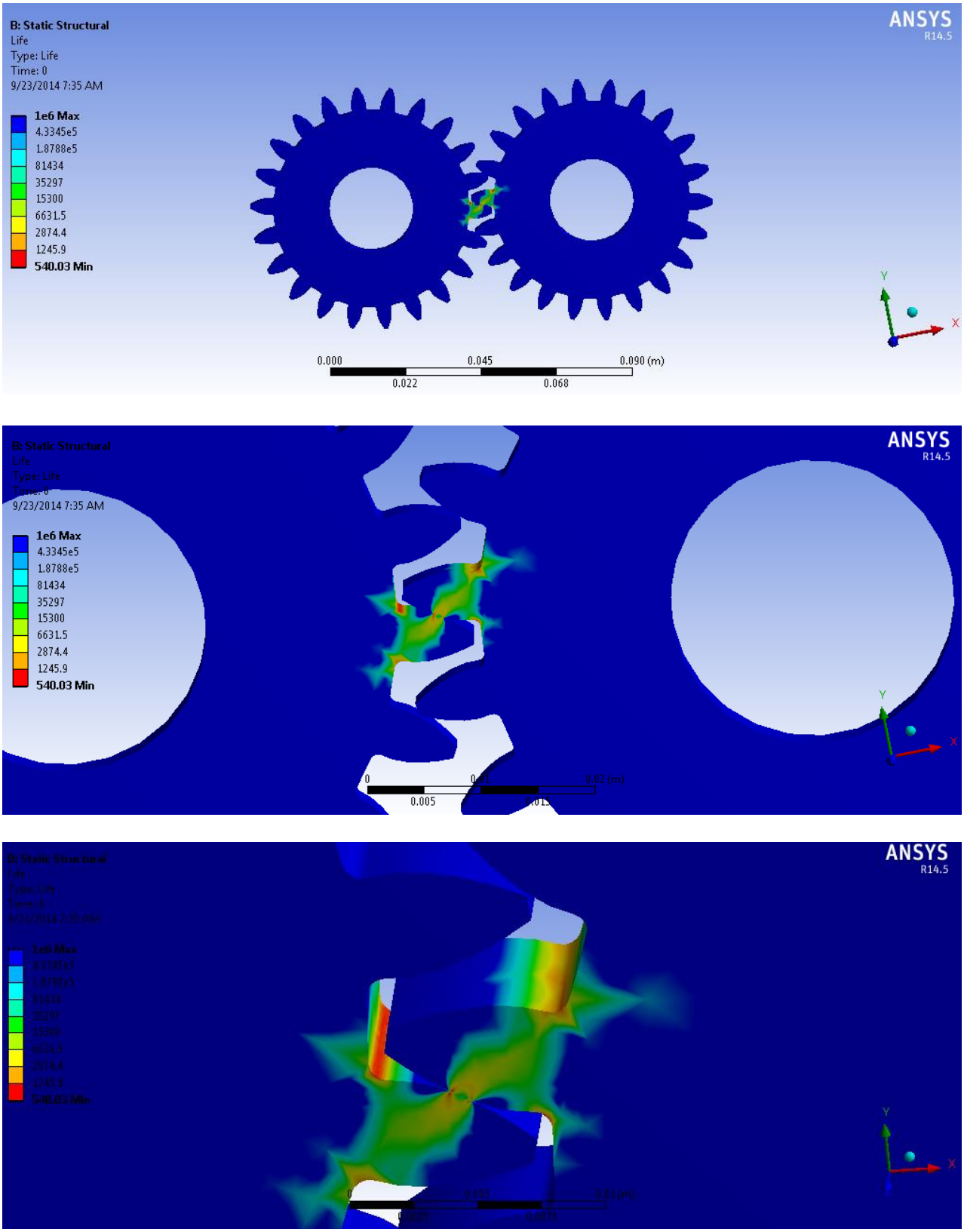

Figure 4.9. Fatigue life analysis by Ansys workbench 14.5

Table 4.5. Surface Fatigue Life estimation for different fatigue strength factor for chromium molybdenum

		Fatigue life in FEM using Max shear stress			
Torque[Nm]	**Fatigue life Ansywork b. using von mises**	**Fatigue strength factor=1**	**Fatigue strength factor=0.9**	**Fatigue strength factor=0.8**	**Fatigue strength factor=0.7**
10	1000000	1000000	831260	421910	197200
15	298460	185980	126900	82597	50608
20	82421	62729	42620	27667	17139
25	34201	26158	1979	11966	7781.8
30	17990	14013	9790.2	6802.7	4502.3
35	9004.1	7908.3	5710.2	3967.8	2626
40	6644	5403.5	3901.6	2711	1825.4
45	4639.8	3795.1	2740.2	1919	1356
50	3404	2803.4	2024.2	1487.3	1051
55	2532.6	2096	1581.9	1164.2	822.8
100	540	449.06	341.44	251.6	178.6

As it is seen in Table 4.5 the Maximum shear stress theory is more conservative than Von mises theory [see also Figure 4.10], hence from now on the Maximum Shear stress criteria will be used.

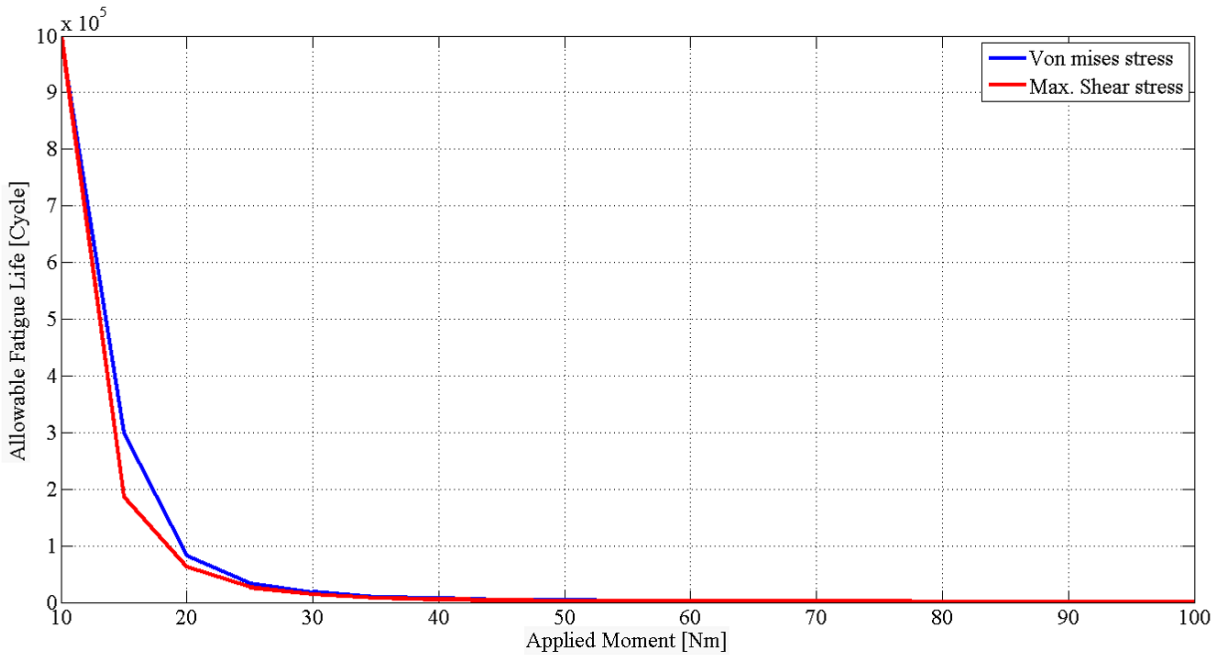

Figure 4.10. Influence of applied load (moment) on Fatigue life Von Mises and Maximum shear stress criteria

The allowable fatigue life for different parts of the involute spur gear is shown in Figure 4.11. a-c.

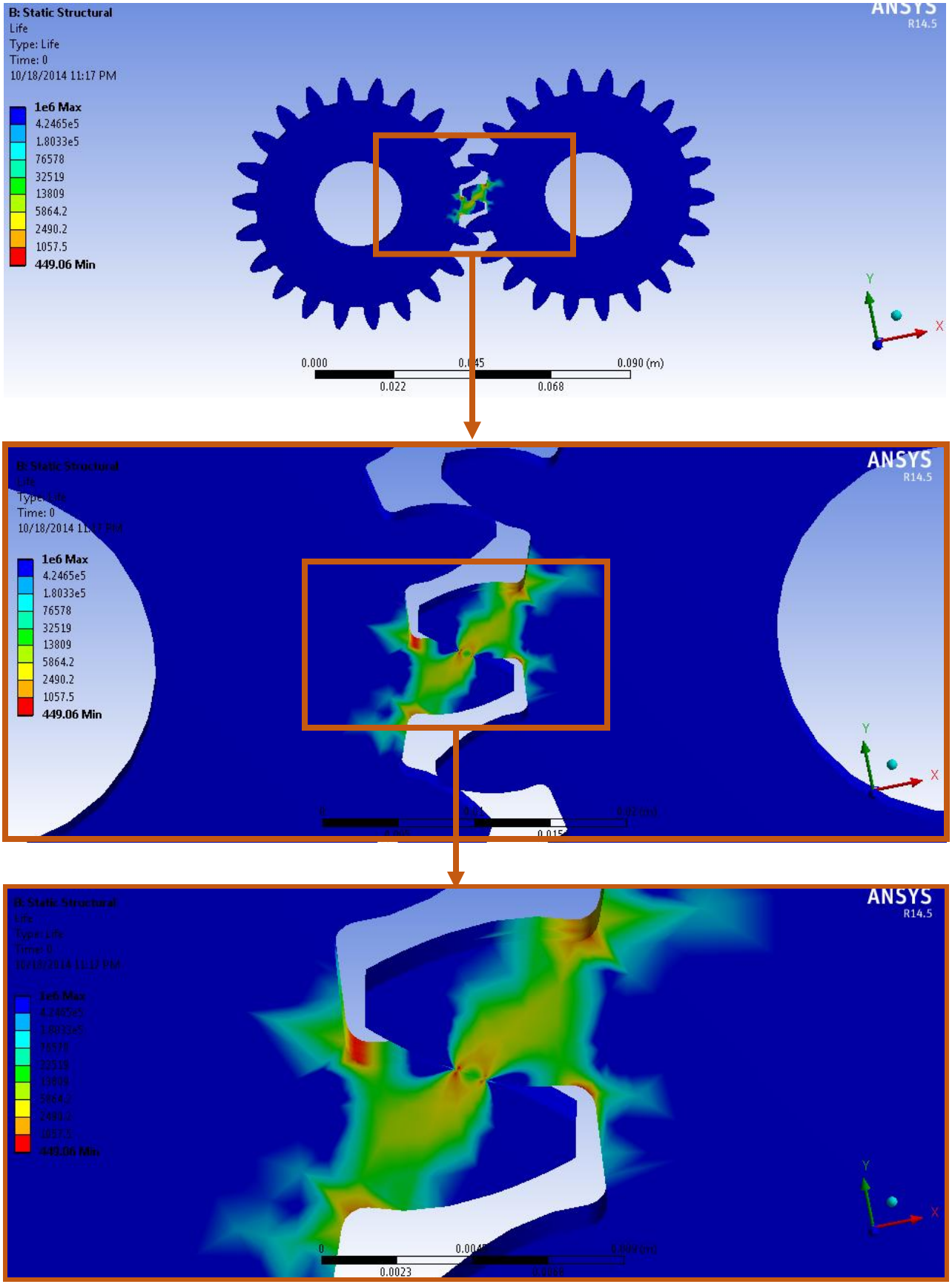
B: Static Structural
Life
Type: Life
Time: 0
10/18/2014 11:17 PM
1e6 Max
4.2465e5
1.8033e5
76578
32519
13809
5864.2
2490.2
1057.5
449.06 Min
ANSYS
R14.5
0.000
0.090 (m)
0.022
0.068
Y
X

Figure 4.11. Fatigue life estimation by FEM with increasing magnification from a to c

The effect of fatigue strength facture on allowable fatigue life is shown in Figure 4.12.

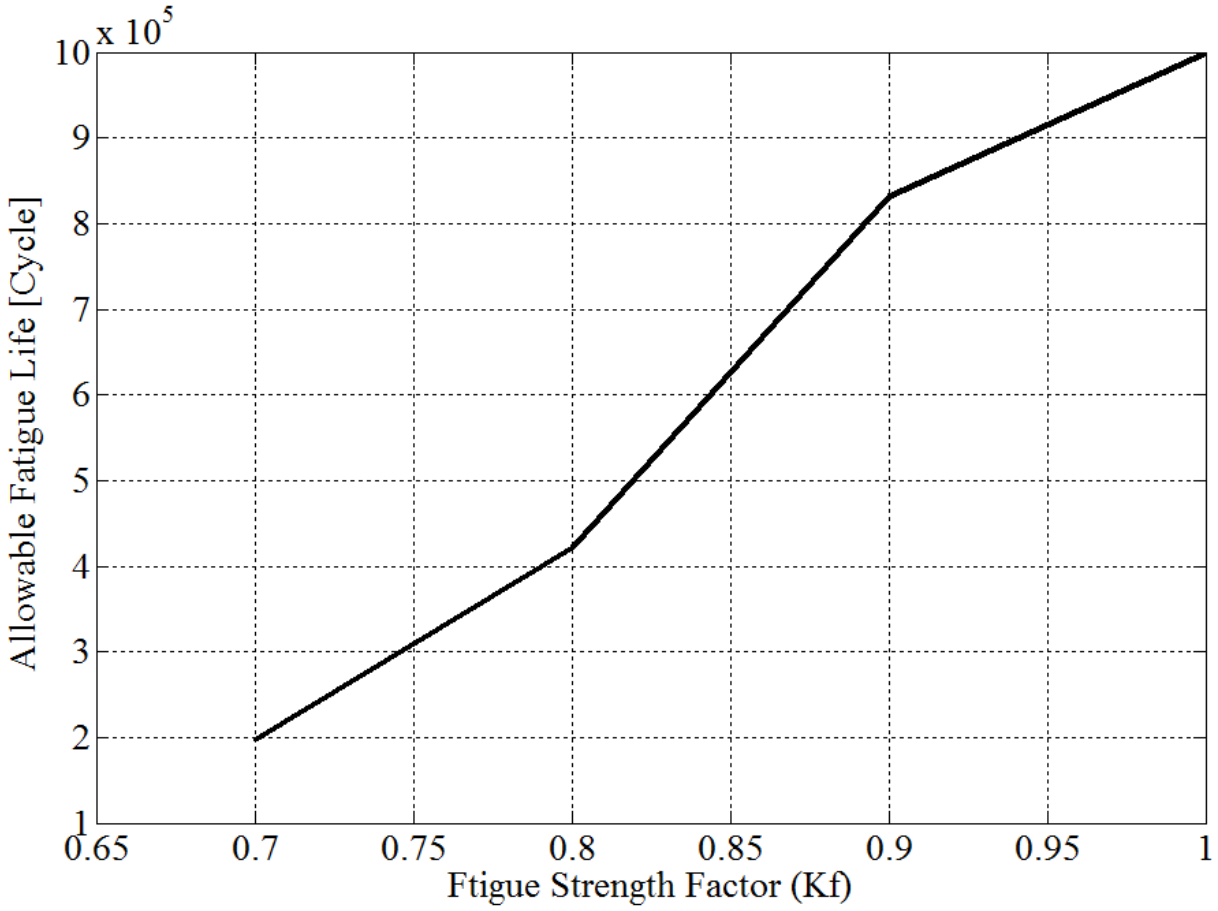

Figure 4.12. Influence fatigue strength factor on fatigue life

The effect of initial surface roughness on surface fatigue life is shown in Figure 4.13. As it is seen in the figure when initial surface roughness increases, the allowable surface fatigue life will reduce significantly.

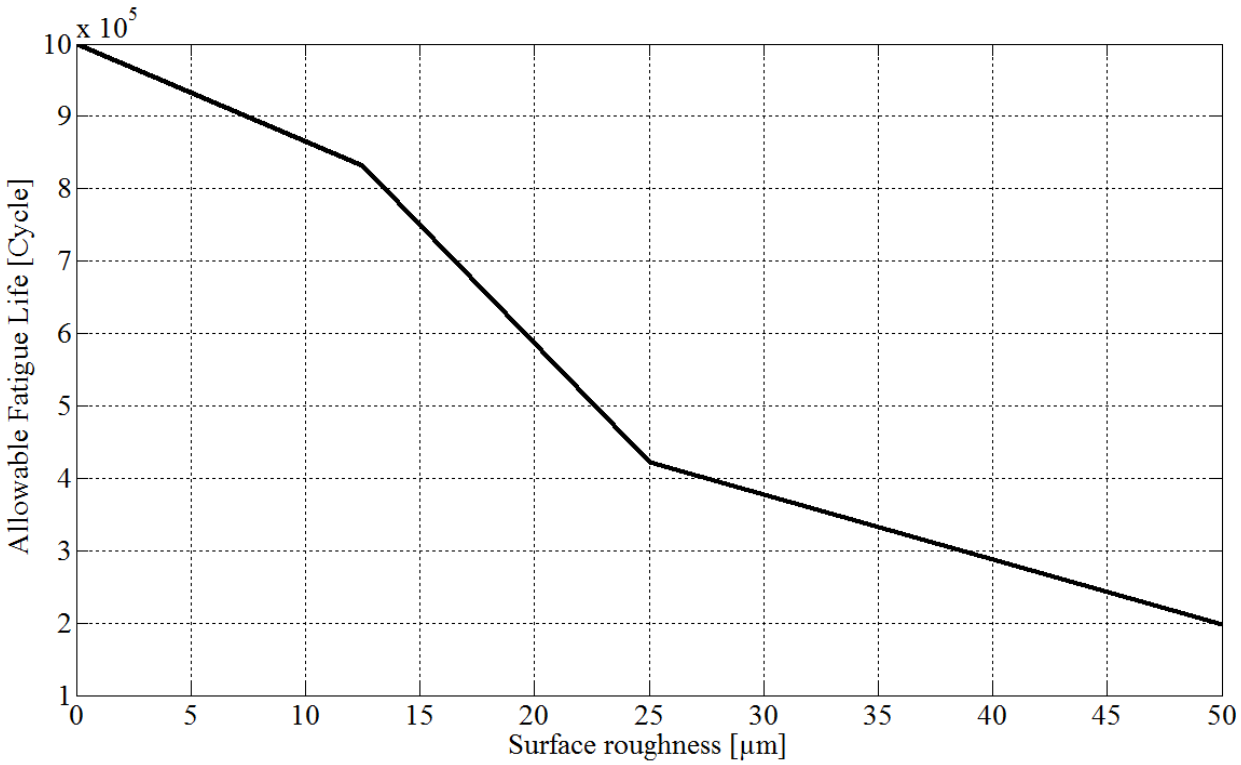

Figure 4.13. Influence of initial surface roughness on surface fatigue life

Finally the surface fatigue life for applied moments varying from 10 to 100Nm with different initial surface roughness is shown in Figure 4.14. As it seen in the figure as the applied load increases the surface fatigue life will decrease for a given initial surface roughness. And for a given applied moment as the initial surface roughness increases the allowable fatigue life reduces significantly specially for lower loads.

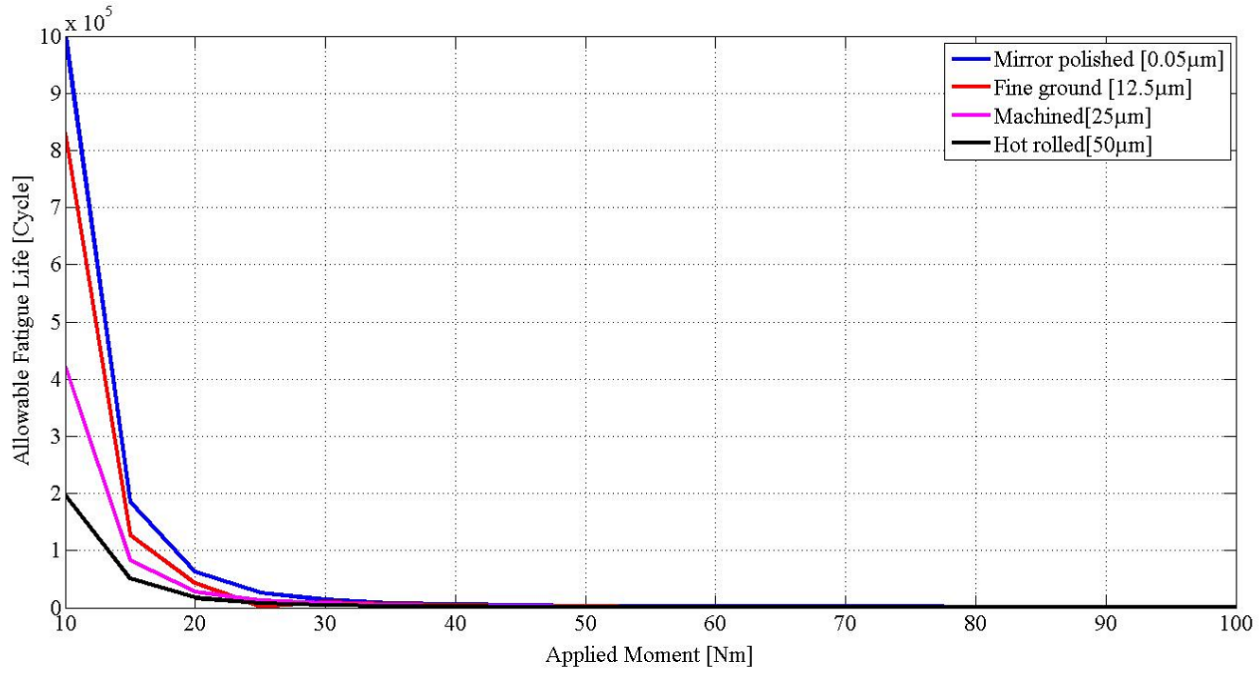

a)

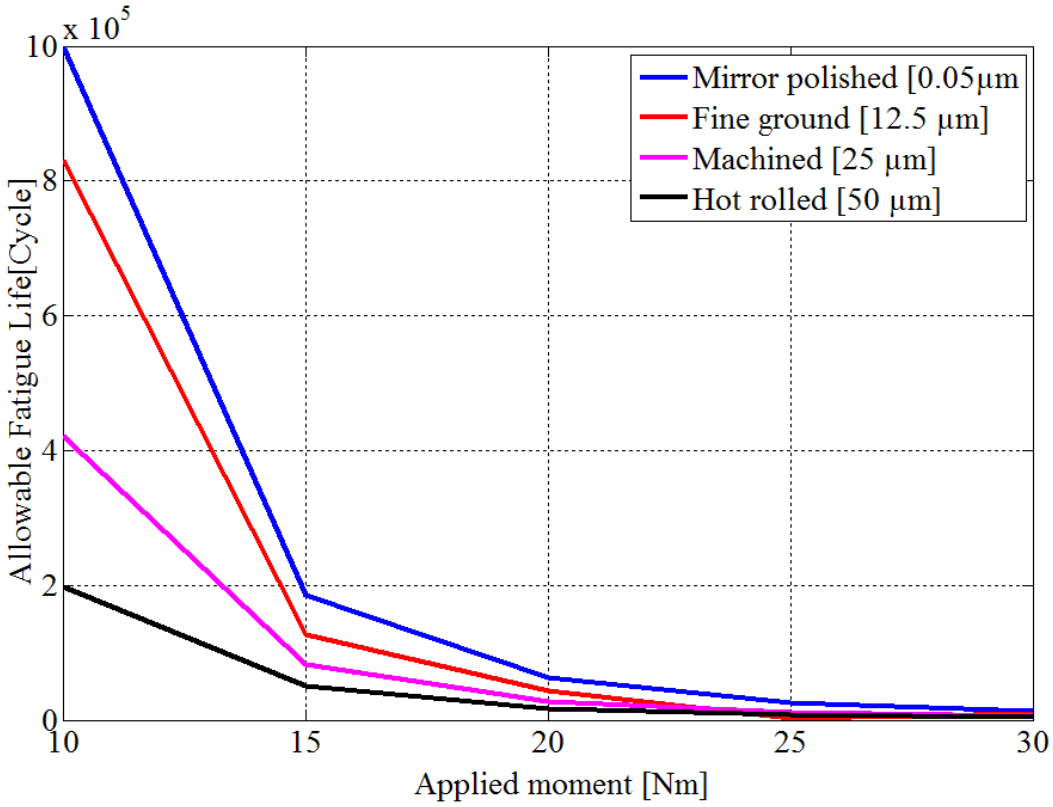

b)

Figure 4.14. Influence of surface finish on fatigue life estimation a) normal scale b) magnified

Chapter Five

5. Conclusion, Recommendation and Future work

5.1. Conclusion

In recent years the application of FEM to different applications is increasing taking the advantage of modernization of computational facilities. In this study the contact stress from Hertezean's stress theory was compared with the contact stress from the FEM was compared and an agreeable result was found. The variation of contact stress with different materials was also compared by using Ansys workbench 14.5. Influence of coefficient of friction on contact stress is analyzed.

And the fatigue life estimation was done using FEM. So we can infer that FEM can be used to analyse contact stress and estimate fatigue life of machine components. Surface fatigue life estimation is performed in FEM ansys workbench 14.5. and the influence of surface finish factor is analyzed.

5.2. Recommendation

Now a days the Finite element method is widely used for mechanical analysis. Using FEM for contact stress analysis and fatigue life estimation have the following advantages: get the solution with reasonable accuracy; requires a short period of time for analysis and less cost as compared to the experimental method. However proper high computational facility is required to get a better result and do the analysis in a more reasonable time.

5.3. Future work

This study has been conducted with miniaturized spur gear pair the FEM analysis was done by an ordinary computer.

- The research has to be done using high computational facility.
- Effect of temperature on fatigue life estimation
- Effect of lubrication on surface fatigue life
- Effect of surface hardness on contact stress/ fatigue life of gears

Reference:

1. Nam H. Kim, Kyle Stoker, A Comparison of Spur Gear Response under Non-Ideal Loading Conditions, SAE, SAE International, Florida.2008.
2. Shigley, Joseph Edward. Mechanical Engineering Design / Joseph E. Shigley, Charles R. Mischke, Richard G. Budynas. – 9th ed.
3. ISO 6336 (1993), Calculation of Load Capacity of Spur and Helical Gears.
4. http://webpages.dcu.ie/~stokesjt/ThermalSpraying/Book/Chapter1.pdf.
5. Bo Alfredsson, AStudy on Contact Fatigue Mechanisim,Doctoral Thesis no. 44, KTH, Stockholm, 2000.
6. Spur Gears, http://www.roymech.co.uk/Useful_Tables/Drive/Gears.html
7. M. Raja Roy, S. Phani Kumar, D.S. Sai Ravi Kiran, Contact pressure analysis of spur gear using FEA, International Journal of Advanced Engineering Applications, Vol.7, Iss.3, pp.27-41 (2014).
8. Santosh S. Patil, Saravanan Karuppanan,Ivana Atanasovska,Azmi Abdul Wahab;Contact stress analysis of helical gear pairs, including frictional coefficients. May 2014, Available online 29 May 2014.
9. Fukuoka Kazuaki, Tomita Kunikazu, Shiraga Tetsuo, Examination of Surface Hardening Process for Dual Phase Steel and Improvement of Gear Properties, JFE Technical Report No. 15 (May 2010).
10. Ravichandra Patchigolla and Yesh P. Singh ; Finite Element Analysis of Large Spur Gear Tooth and Rim With and Without Web Effects-Part I
11. M. Raja Roy, S. Phani Kumar, D.S. Sai Ravi Kiran, Contact pressure analysis of spur gear using FEA, International Journal of Advanced Engineering Applications, Vol.7, Iss.3, pp.27-41 (2014).
12. Gitin M. Maitra; Hand book of gear design 2nd edition,2001.
13. Ali Raad Hassan Ali Raad Hassan , Contact Stress Analysis of Spur Gear Teeth Pair ,World Academy of Science, Engineering and TechnologyVol:3 2009-10-20

14. Parveen Kumar, Harsh Raghuvanshi; Design & Analysis of a Spur Gear in different Geometric Conditions, International Journal of Engineering and Advanced Technology (IJEAT),ISSN: 2249 – 8958, Volume-3, Issue-2, December 2013
15. Vivek Karaveer, Ashish Mogrekar and T. Preman Reynold Joseph, Modeling and Finite Element Analysis of Spur Gear, International Journal of Current Engineering and Technology ISSN 2277 – 4106,2013
16. M. Raja Roy, S. Phani Kumar, D.S. Sai Ravi Kiran, Contact pressure analysis of spur gear using FEA, International Journal of Advanced Engineering Applications, Vol.7, Iss.3, pp.27-41 (2014)
17. Gitin M Maitra, Handbook of gear design, 2nd edition, Tata McGraw-Hill Publishing company limited, 1994.
18. NWM Bishop & F Sherratt, Finite Element Based Fatigue Calculations, UK, July 2000
19. Yung- Li Lee, Richard Hathaway, Mark Barkey; Fatigue Testing and Analysis, Theory and analysis, Elsevier Butterworth-Heinemann,2005
20. Elements of metric gear technology, WWW.SDP-SI.COM,2014.
21. Zienkiewicz, O.C.; Taylor, R.L.; Zhu, J.Z; Finite element Method – its basics and fundamentals
22. Faydor L.Litvin,Alfonso Fuentes; Gear Geometry and Applied Geometry, 2nd edition, Cambridge University Press, 2004.
23. Atul Kumar, P. K. Jain and P. M. Pathak ; Comparative Finite Element Analysis of Reconstructed New and Worn Tooth of Spur Gear , Proceedings of the 1st International and 16th National Conference on Machines and Mechanisms (iNaCoMM2013), IIT Roorkee, India, Dec 18-20 2013.
24. Gang Deng, Tsutomu Nakanishi, Masana Kato, Surface Temperature Calculation and its Application to Surface Fatigue Strength Evaluation, journal of Mechanical Design, December 2002. Vol 124.
25. Amisha Y. Pathak; Computational Approach To Contact Fatigue Damage Initiation And Deformation Analysis Of Gear Teeth Flanks; International Journal of Research in Engineering and Technology, Dec 2012
26. Prof. K.Gopinath & Prof. M.M.Mayuram, Machine Design II, Lecture note on Gears, Indian Institute of Technology Madras.

27. Ravichandra Patchigolla and Yesh P. Singh , Finite Element Analysis of Large Spur Gear Tooth and Rim With and Without Web Effects-Part I , Proceedings of the 2006 ASEE Gulf-Southwest Annual Conference Southern University and A & M College Copyright © 2006, American Society for Engineering Education
28. G. Mallesh,, Dr. V B Math, Gajanan, Uttesh, Sridhar, Estimation of Critical Section and Bending Stress Analysis for Asymmetric Spur Gear Tooth, 14th National Conference on Machines and Mechanisms (NaCoMM09), NIT, Durgapur, India, December 17-18, 2009.
29. Muhsi n J. Jweeg & Wisam Auday Hussain, Contact Stresses for Different Gear Design Parameter , Engineering and Technology journal , Vol 27, No.13, 2009.
30. Timothy Krantz & Brian Tufts, Pitting and Bending Fatigue Evaluations of a New Case-Carburized Gear Steel, NASA/TM—2007-215009.

Appendix I

```
%% Hertizean stress analysis
%% assume the radii of pinion and gear are equal
%% assume the material of the gear and pinion are same
% F is the force applied
%Rp1 and Rp2 are pich radius of pinion and gear respectively
%B is the face width
%phi is the pressure angle
%por1 and por2 is the poisson ratio of pinion and gear respectively
%moe1 and moe2 are the modules of elasticity of pinion and gear
%HCS= hertizean contact stress
%mom=moment applied in Nm
%HCS=sqrt[(F(1+(Rp1/Rp2)))/(Rp1*B*pi*(((1-por1^2)/moe1)+((1-
por2^2)/moe2)*sin(phi))]
%%
closeall
clc
clearall
mo=input('Enter the moment applied :    ');
face_w=input('Enter the face width:    ');
poiss_rp=input('Enter the value of possion ratio of pinoin:    ');
poiss_rg=input('Enter the value of possion ratio of gear:    ');
Ymoe_p=input('Enter the value of youngs modulus of elasticity of pinoin:');
Ymoe_g=input('Enter the value of youngs modulus of elasticity of gear:');
pitch_rad_p=input('Enter the value of pitch radius of pinion :');
pitch_rad_g=input('Enter the value of pitch radius of gear :');
press_angle=input('Enter the value of pressure angle in radian:   ');

mom=mo;
B=face_w;
Rp1=pitch_rad_p;
Rp2=pitch_rad_g;
F=mo/Rp1;
moe1=Ymoe_p;
moe2=Ymoe_g;
por1=poiss_rp;
por2=poiss_rg;
phi=press_angle;

%sample user input values are given below:
% mo=50;
% B=7*10^-3;
% phi=(20/180)*pi;
% Rp1=0.033;
% Rp2=Rp1;
% Ymoe_p=206*10^9;
% Ymoe_g=Ymoe_p;
% poiss_rp=0.3;
% poiss_rg=poiss_rp;
%%
F = mom/Rp1;
HCS = sqrt((F*2)/((Rp1*B*pi)*2*((1-por1^2)/(moe1*1))*sin(phi)));
```

Appendix II

CONTA174 Element Description

CONTA174 is used to represent contact and sliding between 3-D "target" surfaces (TARGE170) and a deformable surface, defined by this element. The element is applicable to 3-D structural and coupled field contact analyses.

The element is located on the surfaces of 3-D solid or shell elements with midside nodes (SOLID87, SOLID90, SOLID98, SOLID122, SOLID123, SOLID186, SOLID187, SOLID226, SOLID227, SOLID231, SOLID232, SHELL132, SHELL281, and MATRIX50).

The element has the same geometric characteristics as the solid or shell element face with which it is connected (see *CONTA174 Geometry* below). Contact occurs when the element surface penetrates one of the target segment elements (TARGE170) on a specified target surface. Coulomb friction, shear stress friction, user defined friction with the USERFRIC subroutine, and user-defined contact interaction with the USERINTER subroutine are allowed. The element also allows separation of bonded contact to simulate interface delamination. See CONTA174 in Appendix III.

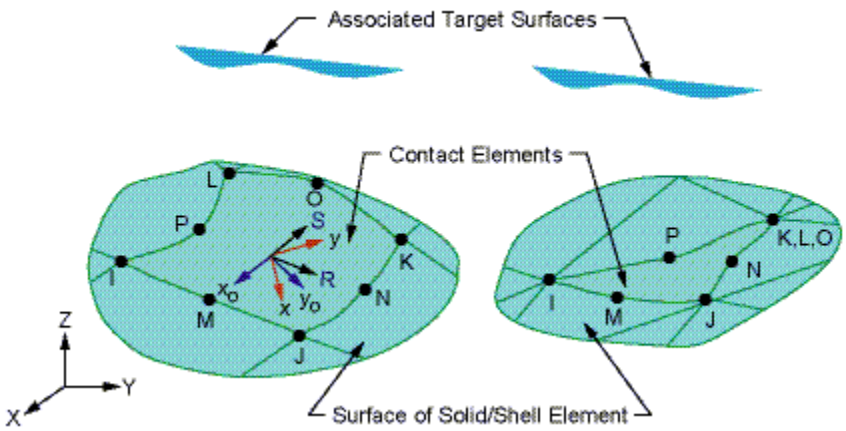

Figure II. CONTA174 Geometry

R = Element x-axis for isotropic friction

x_o = Element axis for orthotropic friction if **ESYS** is not supplied (parallel to global X-axis)

x = Element axis for orthotropic friction if **ESYS** is supplied

Appendix III

TARGE170 Element Description

TARGE170 is used to represent various 3-D "target" surfaces for the associated contact elements (CONTA173, CONTA174, CONTA175, CONTA176, and CONTA177). The contact elements themselves overlay the solid, shell, or line elements describing the boundary of a deformable body and are potentially in contact with the target surface, defined by TARGE170. This target surface is discretized by a set of target segment elements (TARGE170) and is paired with its associated contact surface via a shared real constant set. You can impose any translational or rotational displacement, temperature, voltage, and magnetic potential on the target segment element. You can also impose forces and moments on target elements. See TARGE170 in Appendix II for more details about this element. To represent 2-D target surfaces, use TARGE169, a 2-D target segment element.

For rigid target surfaces, these elements can easily model complex target shapes. For flexible targets, these elements will overlay the solid, shell, or line elements describing the boundary of the deformable target body.

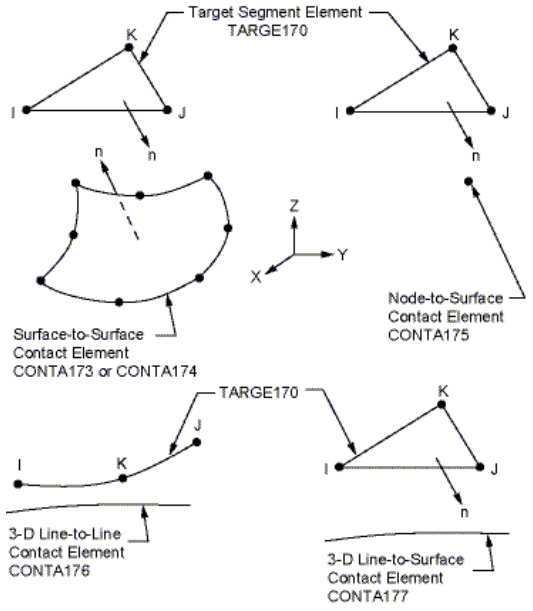

Figure III: TARGE170 Geometry